5. Equatorial waves

Because the atmosphere has in general a better homogeneity in the longitudinal (zonal or rotating) direction, it is quite reasonable to expand any meteorological quantity or forcing term (such as insolation) into a Fourier series as waves with various zonal wavenumbers and frequencies (or their ratios or zonal phase velocities). The zonal mean of such a wave component itself becomes zero, just as defined as a disturbance or an eddy in (4.1). A nonlinear quadratic term does not vanish even if the zonal mean is taken, but it is negligible in the first-order approximation (so almost linear) if the amplitude of the wave component is sufficiently small. Such a linear problem can be solved relatively easily by the Fourier expansion. For a global approach on the spherical Earth it is requested to use a spherical polynomial or Legendre expansion, but for a study near the equator a cylindrical (Bessel. Hermite, etc.) function expansion or even the simplest Fourier expansion becomes sufficiently useful approximation. Those techniques of mathematics to solve wave equations and of data calculations to analyze wave components have been prepared sufficiently for applications in many scientific fields, which is practically convenient background for applying the wave concepts to the tropical meteorology and climatology.

More importantly than practical, in the general fluid dynamics any waves must have concrete restoring forces (such as buoyancy, vorticity conservation, and compressibility) and amplifying mechanisms (forcing sources, instabilities, and free normal modes) determined by characteristics and conditions of the considered fluid system. Therefore, if a phenomenon is proved to be associated with a wave, we may clarify its cause in past and may predict its reoccurrence in future, although nonlinearity (multiple wave interactivity) and irreversibility (transience, dissipation, etc.) make difficulty. Furthermore fluid waves transport energy and momentum without direct circulations (mass transport), just like electromagnetic waves (cf. Chapter 1) in vacuum space, by which tropical regionally excited waves may cause global extratropical abnormal weather/climate, and waves excited in the troposphere may (interact the mean flow and) induce non-diurnal non-annual oscillations of the middle and upper atmospheres.

In spite of such importance the history of wave dynamics in the tropics is very young, almost only during the recent half century. It is clearly because the equatorial region has special situations such as vanishing Coriolis force, strong insolation, high moisture, interaction with the ocean broader than the northern mid latitudes, and so on, which generates special kinds of 'equatorial waves' to be described in this chapter. In addition many regions in the tropics have not been observed well until few decade ago, because of unstable politics, slow economic development, and/or insufficient measuring technology. However, in particular economic/political situations the south and southeast Asian countries, as well as fully global satellite remote sounding technologies, have been developed very rapidly. High resolution atmosphere-ocean coupled models also have been constructed. Now we are starting to study the global atmosphere including the tropics almost seamlessly.

5.1. Classification of waves in geophysical fluids

Subtracting the zonal mean equations (4.2)−(4.6) from the basic equations (3.13)−(3.17), we obtain

$$\frac{\overline{D}u'}{Dt} + \left(\frac{\partial \overline{u}}{\partial y} - f\right)v' + \frac{\partial \overline{u}}{\partial z}w' + \frac{\partial \phi'}{\partial x} = G_x{'}, \qquad (5.1)$$

$$\frac{\overline{D}v'}{Dt} + fu' + \frac{\partial \phi'}{\partial y} = G_y', \tag{5.2}$$

$$\frac{\partial \phi'}{\partial z} = \frac{RT'}{H}, \tag{5.3}$$

$$\frac{\overline{D}T'}{Dt} + \frac{\partial \overline{T}}{\partial y}v' + \left(\frac{\partial \overline{T}}{\partial z} + \Gamma\right)w' = Q', \tag{5.4}$$

$$\frac{\partial u'}{\partial x} + \frac{\partial v'}{\partial y} + \frac{1}{\rho_0}\frac{\partial \rho_0 w'}{\partial z} = 0, \tag{5.5}$$

where we have assumed the mean flow only in the zonal direction for simplicity:

$$\frac{\overline{D}}{Dt} \equiv \frac{\partial}{\partial t} + \overline{u}\frac{\partial}{\partial x}, \tag{5.6}$$

and have summarized all the nonlinear terms and non-axisymmetric forcing terms into G_x', G_y' and Q'.

As the simplest case, we assume also that the meridional and vertical shears of the mean flow are sufficiently weak ($\partial \overline{u}/\partial y \approx \partial \overline{u}/\partial z \approx 0$; then automatically $\partial \overline{T}/\partial y \approx 0$ by the thermal-wind equilibrium (4.11)), apply the equatorial β-plane approximation (4.7) and the Vaisala-Brunt frequency expression for vertical temperature gradient (4.19), and almost free conditions (sufficiently far away from any boundaries and weak internal forcing/dissipation; then $G_x' \approx G_y' \approx Q' \approx 0$). In this case (5.3)–(5.5) may be summarized into one (so-called shallow-water) equation:

$$-\frac{1}{N^2 \rho_0}\frac{\overline{D}}{Dt}\frac{\partial}{\partial z}\rho_0\frac{\partial \phi'}{\partial z} + \frac{\partial u'}{\partial x} + \frac{\partial v'}{\partial y} = 0. \tag{5.7}$$

Thus our problem is to solve three equations (5.1), (5.2) and (5.7) for three dependent variables u', v' and ϕ'.

Assuming the factors of those three equations are strongly dependent only on y, we may put sinusoidal forms (as in the Fourier expansion) concerning x, z and t dependencies:

$$\begin{pmatrix} u' \\ v' \\ \phi' \end{pmatrix} \equiv e^{z/2H} \cdot \Re\left[\begin{pmatrix} \tilde{u}(y) \\ \tilde{v}(y) \\ \tilde{\phi}(y) \end{pmatrix}\exp\{i(kx + mz - \omega t)\}\right], \tag{5.8}$$

where $\Re[\ ]$ denotes to take the real part, k and m are zonal and vertical wavenumbers, and ω is frequency (relative to the ground). A factor dependent on $e^{z/2H}$ implies that the wave is automatically amplified upward to compensate the decrease of atmospheric density ρ_0 to conserve the wave energy $\propto \rho_0 \cdot |\text{amplitude}|^2$. Substituting (5.8) into (5.1), (5.2) and (5.7) and using the 'intrinsic' frequency relative to the wave media moving with the mean flow $\overline{u}$:

$$\hat{\omega} \equiv \omega - k\overline{u}, \tag{5.9}$$

we obtain a set of ordinary differential equation only for y:

$$\begin{pmatrix} -i\hat{\omega} & -\beta y & ik \\ \beta y & -i\hat{\omega} & d/dy \\ ik & d/dy & -i(\hat{\omega}/N^2)(m^2 + 1/4H^2) \end{pmatrix} \cdot \begin{pmatrix} \tilde{u}(y) \\ \tilde{v}(y) \\ \tilde{\phi}(y) \end{pmatrix} = 0,$$

which may be reduced to the following single equation only for one dependent variable $\tilde{v}$:

$$\frac{d^2\tilde{v}}{dy^2} + \left[\left\{\left(m^2 + \frac{1}{4H^2}\right)\frac{\hat{\omega}^2}{N^2} - k^2 - \frac{k\beta}{\hat{\omega}}\right\} - \frac{\beta^2}{N^2}\left(m^2 + \frac{1}{4H^2}\right)y^2\right]\tilde{v} = 0. \tag{5.10}$$

$$\Psi_n(y/\lambda_e)/\sqrt{2}^n\sqrt{2\pi} \propto e^{-y^2/2\lambda^2} \cdot H_n(y/\lambda);$$
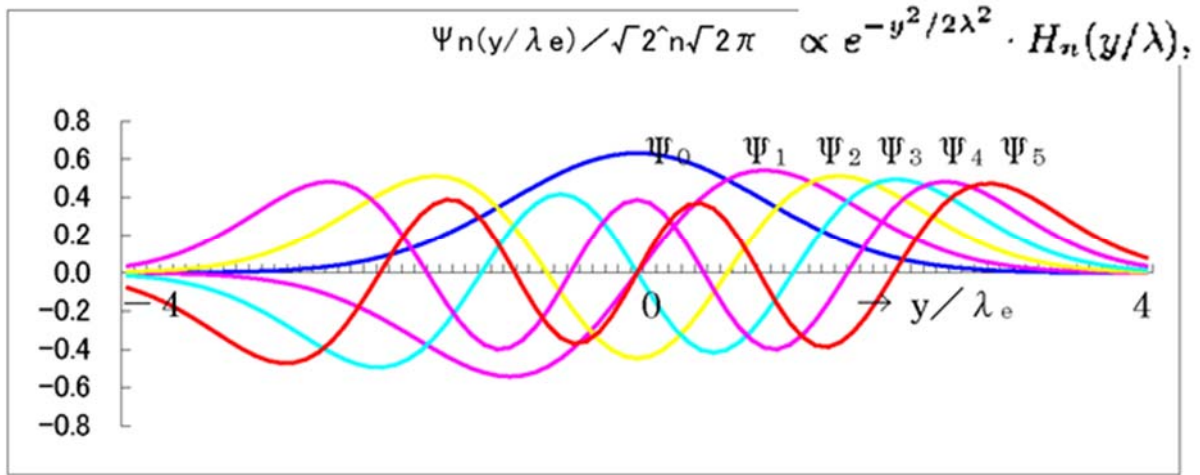
Fig. 5.1 The Hermite polynomials as the meridional structure function of the equatorial shallow water wave equations.

Then the other two variables are obtained from $\tilde{v}$ and its derivative as follows:

$$\tilde{u} = i\frac{kd\tilde{v}/dy - [(m^2 + 1/4H^2)\widehat{\omega}\beta y/N^2]\tilde{v}}{k^2 - (m^2 + 1/4H^2)\widehat{\omega}^2/N^2}, \quad \tilde{\phi} = i\frac{\widehat{\omega}d\tilde{v}/dy - k\beta y\tilde{v}}{k^2 - (m^2 + 1/4H^2)\widehat{\omega}^2/N^2}, \qquad (5.11)$$

which are called the *polarization relations*. Although earlier studies to solve essentially similar problems (such as tides) used another single equation for $\tilde{\phi}$ with a more complex form, Matsuno (1966) derived (5.9) which was a breakthrough to obtain many important features describe in this section. Almost simultaneously but completely independently Kato (1966) and also Lindzen (1966) noticed that the depth h of truly shallow water (ocean) in the classical tidal theories[37] could be related to the vertical wavenumber as

$$gh = N^2\left(m^2 + \frac{1}{4H^2}\right)^{-1}, \qquad (5.12)$$

which could take a negative value for the atmosphere, in case of *external* (upward decaying) modes with imaginary wavenumbers $m = im_i$. The *internal* modes (vertically propagating waves) are labeled by real numbers of m and positive numbers of h. Later we see that for example gravity waves with the diurnal period (related to global tides and local diurnal cycles) are internal and external in the latitudes lower and higher than 30º. An estimation[38] for waves considered here is $h \sim 100$ m, corresponding to a vertical wavelength $2\pi/m \sim 10$ km.

Matsuno (1966) solved (5.10) for a boundary condition:

$$|\tilde{v}| \to 0 \quad \text{for} \quad y \to \pm\infty,$$

corresponding to solutions decaying poleward[39], i.e., trapped near the equator, requested also from the mathematical validity of equatorial β-plane approximation. If a homogeneous equation such as (5.10) has a nontrivial solution (other than $\tilde{v} \equiv 0$) satisfying arbitrary boundary conditions, the factor of the equation must have a special form, namely the bracket { } must take certain values which are called eigenvalues. Fortunately (5.10) is mathematically equivalent to the Hermite equation appeared in quantum mechanics, and the so-called eigensolutions

---

[37]In the classical tidal theories for the atmosphere, the vertical structure was obtained from (5.7) by separating variables, in which h was used as the separation constant and called '*equivalent depth*'.

[38]The earliest estimation $h \sim 10$ km was carried out in 1930s based on records of pressure disturbances caused by Krakatau (Krakatoa) eruption in 1883 (cf. Fig. 1.8), but this was due to a special case of acoustic-gravity waves (Lamb wave) filtered out in our basic equations.

[39]The both poles are located at $y = \pm\infty$ in the equatorial β-plane approximation (4.7).
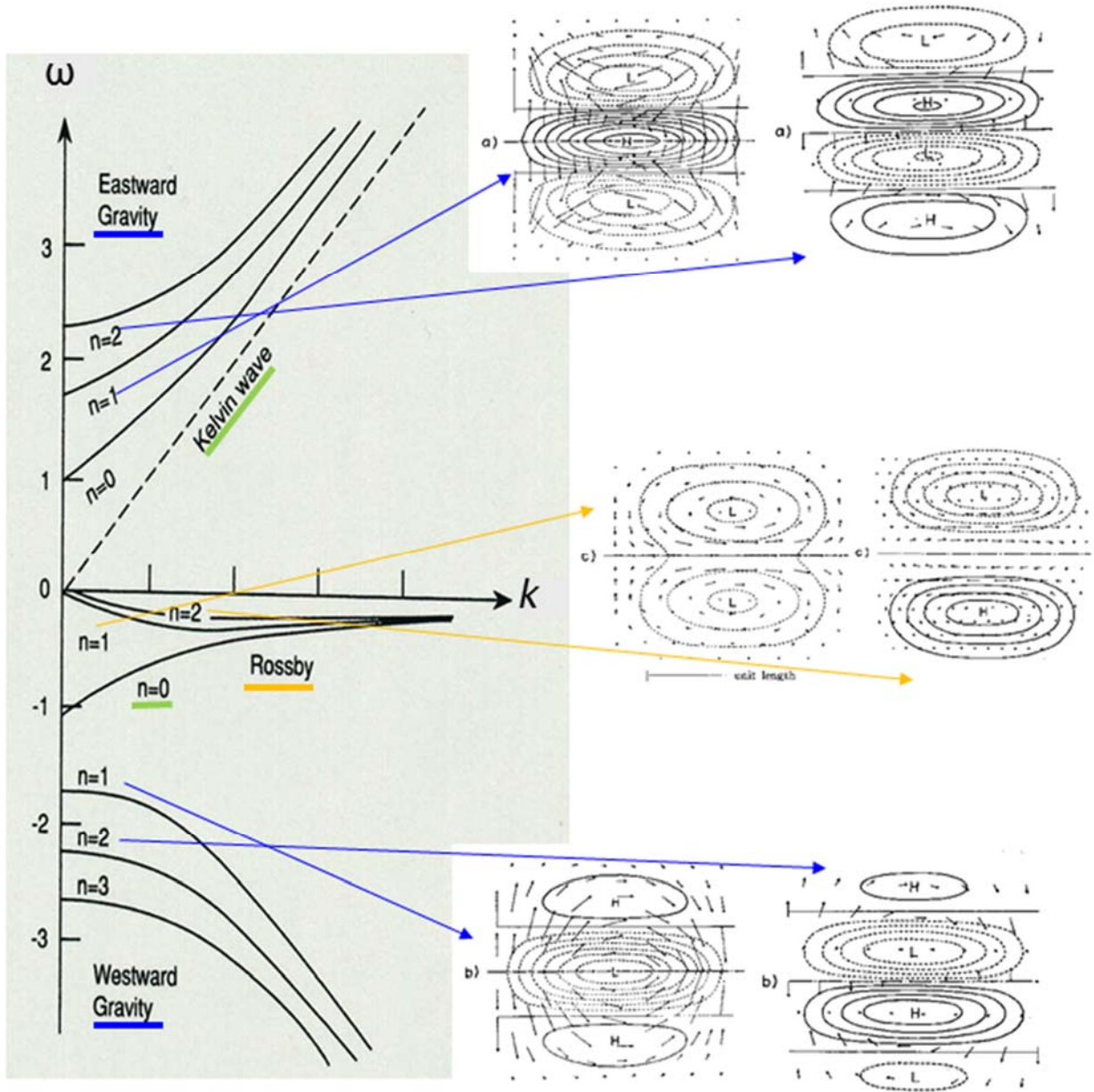
Fig. 5.2 The dispersion (frequency–zonal wavenumber) diagram of shallow-water-approximated equatorially trapped waves solved by Matsuno (1966) with horizontal structures of inertio-gravity and Rossby modes.

satisfying that boundary condition had been known already:

$$\tilde{v}(y) \propto e^{-y^2/2\lambda^2} \cdot H_n(y/\lambda), \qquad \lambda = \left[\frac{N^2}{\beta^2} \Big/ \left(m^2 + \frac{1}{4H^2}\right)\right]^{1/4}, \tag{5.13}$$

where λ is the equatorial deformation radius (4.21) for h given by the equivalent depth (5.12), and $H_n(y/\lambda)$ is the nth-degree Hermite polynomials for argument y/λ (see Fig. 5.1). For $h{\sim}100$ m, the equivalent shallow-water gravity-wave phase speed $\sqrt{gh}{\sim}30$ m/s${\sim}2{,}600$ km/day, and the deformation radius $\lambda = (gh/\beta^2)^{1/4}{\sim}1{,}000$ km $\sim$ 10° latitude. The eigenvalues providing appropriate solutions are

$$\lambda^2 \left(\frac{\widehat{\omega}^2}{\lambda^4\beta^2} - k^2 - \frac{k\beta}{\widehat{\omega}}\right) = 2n + 1 \qquad (n = 0, 1, 2, \cdots), \tag{5.14}$$

which may be plotted in the $\widehat{\omega}$-k plane as shown in Fig. 5.2. A formula such as (5.14) concerning the wave parameters (k, m and ω in this case) is called the *dispersion relation*, and is mathematically given also by a simple replacement rule such as $(\partial/\partial x,\ \partial/\partial z,\ \partial/\partial t) \rightarrow i(k, m, -\omega)$ in the factor of governing equation (5.10) or those of the original ones (5.1)−(5.5), as well as a formal expression of *local wavenumber* considering an approximate wavelike solution $\tilde{v}(y) \propto e^{ily}$ for the meridional direction:

$$l(y)^2 = \frac{2n+1}{\lambda^2} - \frac{y^2}{\lambda^4}. \tag{5.15}$$

Therefore the dispersion relation includes the field (wave media) parameters (β, N, H, $\overline{u}$ in this case) given in factors of the governing equations, and determine the basic structures of waves as the solutions.

The factor $e^{-y^2/2\lambda^2}$ multiplied on the whole solutions (5.13) shows a rapid decay of wave amplitude away from the equator, by which we confirm very easily that the solutions satisfy the boundary condition. (5.15) implies that the eigenvalue number n represents the meridional wave structure (more exactly speaking, the number of nodes of the meridional velocity $\tilde{v}$ profile in the meridional direction), and such a wavelike variation (with a real value of l) is restricted within $|y| < \sqrt{(2n+1)}\lambda$, which may be confirmed by plotting the Hermite function[40] $H_n(y/\lambda)$:

$$H_0\left(\frac{y}{\lambda}\right) = 1, \qquad H_1\left(\frac{y}{\lambda}\right) = 2\frac{y}{\lambda}, \qquad H_2\left(\frac{y}{\lambda}\right) = 4\left(\frac{y}{\lambda}\right)^2 - 2, \qquad H_3\left(\frac{y}{\lambda}\right) = 8\left(\frac{y}{\lambda}\right)^3 - 12\frac{y}{\lambda}, \quad \cdots.$$

From these considerations we understand that the equatorial deformation radius λ is essential to define the horizontal scale of tropical wave dynamics.

The dispersion relation (5.14) is a cubic equation (with at maximum three roots) for $\widehat{\omega}$, when all the other wave and field parameters are completely given. This number of roots is originated by the number of time derivatives appeared in the basic equations (5.1)−(5.5)[41], and the three roots are those corresponding to eastward and westward moving (inertio-) gravity waves, and westward moving Rossby (planetary) waves. Namely, if we take a limit $\beta \rightarrow 0$, (5.10) and (5.13)−(5.15) are reduced to those for the shallow-water gravity waves without Earth's rotation (Fig. 5.3):

$$\frac{d^2\tilde{v}}{dy^2} + \left[\left(m^2 + \frac{1}{4H^2}\right)\frac{\widehat{\omega}^2}{N^2} - k^2\right]\tilde{v} = 0, \quad \lambda \rightarrow \infty, \quad \left(m^2 + \frac{1}{4H^2}\right)\frac{\widehat{\omega}^2}{N^2} - k^2 = l^2.$$

Alternatively, if $h \rightarrow \infty$, namely $m^2 + 1/4H^2 \rightarrow 0$, we have a Rossby wave with no horizontal divergence:

$$\frac{d^2\tilde{v}}{dy^2} - \left(k^2 + \frac{k\beta}{\widehat{\omega}}\right)\tilde{v} = 0, \qquad \lambda \rightarrow \infty, \qquad -\frac{k\beta}{\widehat{\omega}} - k^2 = l^2.$$

These are too extreme, no restriction for the tropics ($\lambda \rightarrow \infty$), and almost continuous spectral band (n disappeared).

More realistic approach is to classify cases by temporal scales, i.e., the magnitude of $|\widehat{\omega}|$. On one hand, if the temporal scale is so short as to neglect the last term in the bracket of (5.14), i.e., $|\widehat{\omega}| \gg \beta/k$,

$$\widehat{\omega}^2 - \beta^2 y^2 \approx \frac{k^2 + l(y)^2}{m^2 + 1/4H^2}N^2, \tag{5.16}$$

which is known as the dispersion relation for *inertio-gravity waves* (Fig. 5.4), applied for the equatorial β-plane. The frequency of internal (vertically propagating) modes with real vertical wave numbers ($m^2 > 0$) must satisfy

---

[40]The definition of the Hermite polynomials has a variety. Here we use $H_n(x) \equiv (-1)^n \cdot e^{x^2} \cdot d^n e^{-x^2}/dx^n$.

[41]The original forms of the basic equations (three components (2.3), and (2.4)−(2.5)) have time derivatives, and there may be five roots for $\widehat{\omega}$ corresponding to five modes: Rossby, two gravity and two acoustic waves. The last two roots are omitted in meteorology, by neglecting the time derivatives in the vertical momentum (hydrostatic) and continuity equations (Boussinesq) as in (5.1)−(5.5).
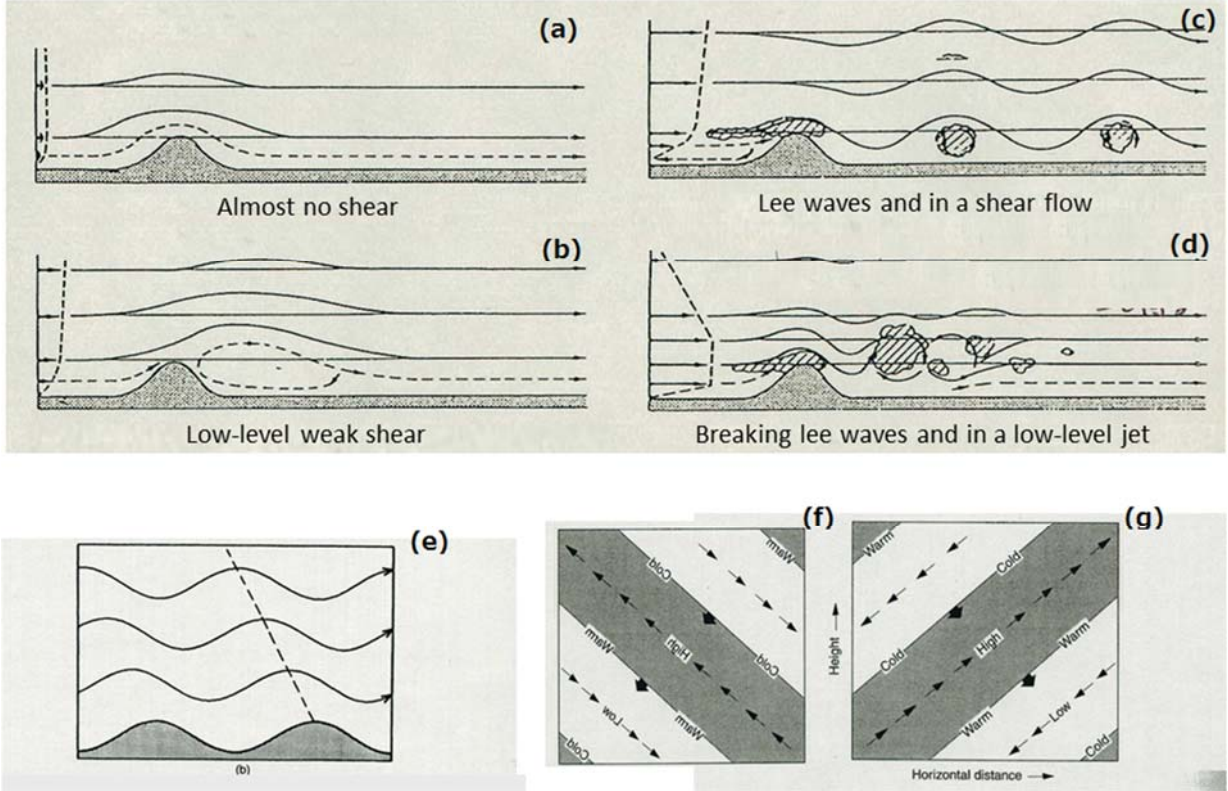
Fig. 5.3 Internal gravity waves (without the inertial (Earth's rotation) effect): (a)−(d) mountain (lee-side) waves for various flows (Corby, 1954); (e) internal waves in a shear flow (Durran, 1990); and (f) −(g) phae structures in the vertical plane including the propagation direction for k and m with the same sign and opposite signs (Holton, 1992).

$$|f|(= |\beta y|) < |\widehat{\omega}| < N.$$

These waves may propagate in any horizontal directions dependent on signs/values of k, l $[= \sqrt{(2n+1)}/\lambda$ at the equator $y = 0]$ and ω, and their 'horizontal' phase speeds relative to the media moving with the mean zonal velocity $\overline{u}$ are commonly given at the equator as

$$\left|\frac{\widehat{\omega}}{\text{horizontal wavenumber}}\right| = \sqrt{\frac{\widehat{\omega}^2}{k^2 + l(y)^2}} \approx \sqrt{\frac{N^2}{m^2 + 1/4H^2}} = \sqrt{gh},$$

which is just the same as gravity waves in a shallow water with mean depth h. Positive/negative roots $\pm|\widehat{\omega}|$ for a given set of the other parameter values correspond to waves propagating symmetrically eastward/westward relative to the media. The frequency ω and zonal phase velocity ω/k relative to the ground are not symmetric. In other words, in the basic flow, waves propagating eastward/westward with the same speed have different values of $|\widehat{\omega}|$, and hence different structures and characteristics, which are essentially important in the wave-mean flow interactions (Section 5.4). Although detailed description of waves common also in the extratropics is out of the scope, it may be shown from (5.11), (5.16) and (5.8) that the perturbed horizontal velocity $\boldsymbol{u}'_H \equiv (u', v')$ makes an elliptic oscillation of which the long axis directs the horizontal propagation direction (parallel to the horizontal wavenumber: $\boldsymbol{k}_H \equiv (k, l)$ $(k, l))$[42]; the short/long axis ratio is $|f/\widehat{\omega}|$ $(= |\beta y/\widehat{\omega}|)$, and the rotation direction is the same as f (=

---

[42]The easiest confirmation is done for a zonal propagation mode ($l = 0$, $d/dy = 0$): from (5.16) $k^2 - (m^2 + 1/4H^2)\widehat{\omega}^2/N^2 \approx -(m^2 + 1/4H^2)f^2/N^2$, and (5.10) becomes , $\tilde{u} = i(\widehat{\omega}/f)\tilde{v}$, $\tilde{\phi} = i[k/\{(m^2 + 1/4H^2)f/N^2\}]\tilde{v} = [kN^2/\{\widehat{\omega}(m^2 + 1/4H^2)\}]\tilde{u}$.
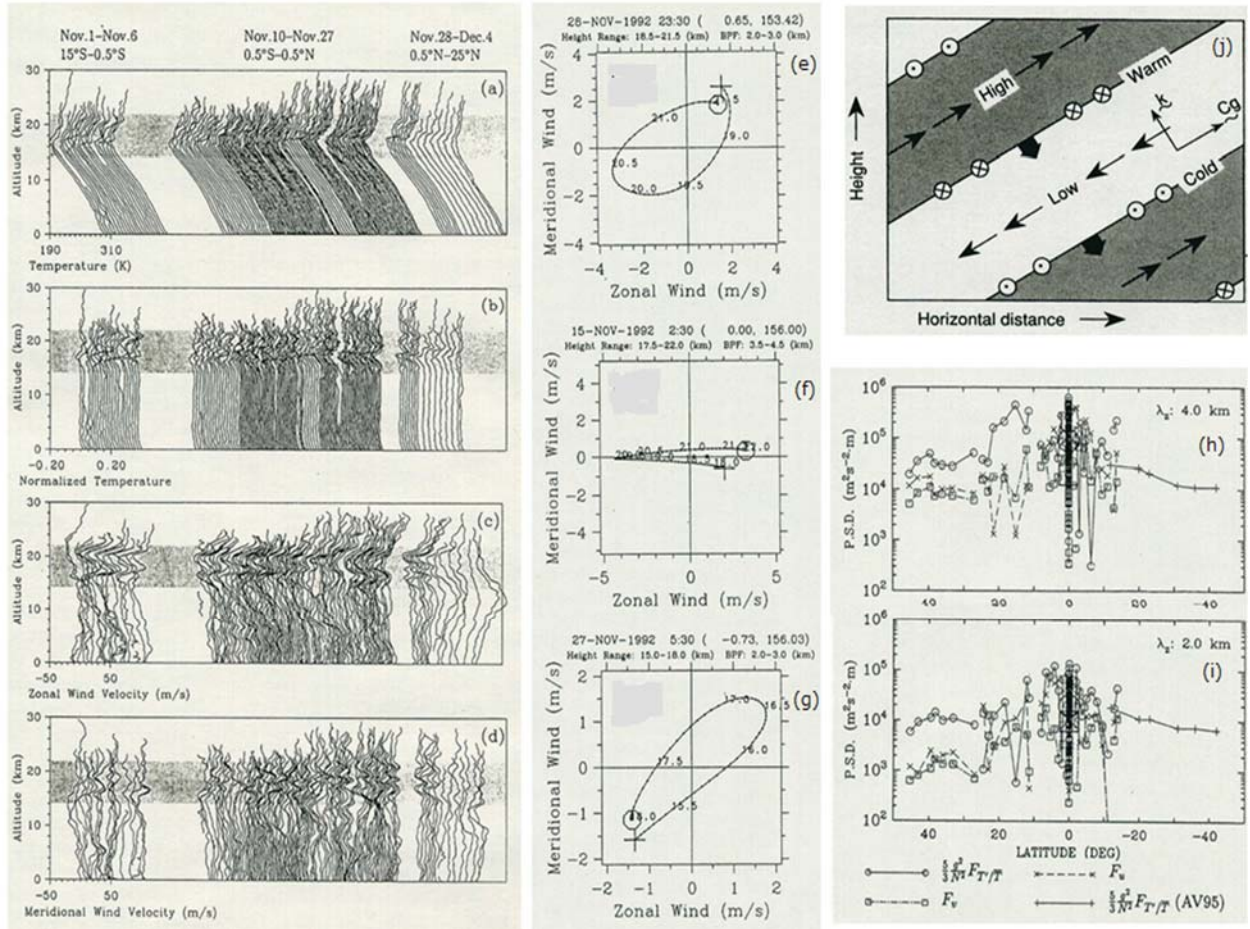
58

Fig. 5.4 Inertio-gravity waves: intensive radiosonde observations in around the tropics (Ogino et al., 1995) for (a)−(d) temperature and its normalized anomaly, and zonal and meridional winds; (e)−(g) horizontal wind vector hodographs in the northern hemisphere, at the equator and in the southern hemisphere; and (h)−(i) meridional distributions of amplitudes of 4 and 2 km vertical wavelength modes. In addition (j) is theoretical phase structure (Holton. 1992).

βy). It becomes a linear oscillation at the equator ($f = 0$), and becomes an inertial circular motion if the frequency t akes the lowest limit ($|\hat{\omega}| \to |f|$). It is also shown that ϕ' and the long-axis component of wind are in or anti phase, and $\phi' \approx \hat{\boldsymbol{c}}_{\mathrm{H}} \cdot \boldsymbol{u}'_{\mathrm{H}}$ for $f \approx 0$, where $\hat{\boldsymbol{c}}_{\mathrm{H}} \equiv (\hat{\omega}/|\boldsymbol{k}_{\mathrm{H}}|^2)\boldsymbol{k}_{\mathrm{H}}$ is the horizontal phase velocity relative to the media.

On the other hand, if the temporal scale is so long as to neglect the first term in the bracket of (5.14), i.e.,$|\hat{\omega}| \ll N$, we have a dispersion relation for *shallow-water Rossby waves* (Fig. 5.5) over the equatorial β-plane:

$$\hat{\omega} \approx \frac{-k\beta}{k^2 + l(y)^2 + (\beta^2 y^2/N^2)(m^2 + 1/4H^2)}. \tag{5.17}$$

This wave does not exist if $\beta = 0$ (homogeneous or no rotation), and $\hat{\omega} \to -0$ in the limit of $k \to 0$. The zonal phase propagation direction is always westward. Because of small $|\hat{\omega}|$ (corresponding to $|\overline{D}/Dt|$), (5.11) becomes approximately geostrophic: $\tilde{v} \approx i(k/\beta y)\tilde{\phi}$ and $\tilde{u} \approx -(l/k)\tilde{v} \approx -i(l/\beta y)\tilde{\phi}$. There are many good textbooks in which these two classical types of waves are explained in more details (e.g., Holton, 1992; Gill, 1982; Andrews, 2000).

It is for $n \geq 1$ that the general dispersion relation (5.14) with (5.15) has three roots for $\hat{\omega}$, corresponding to those inertio-gravity and Rossby waves common to the extratropics. For $n = 0$ (in this case $\tilde{v}(y) = e^{-y^2/2\lambda^2}$ has
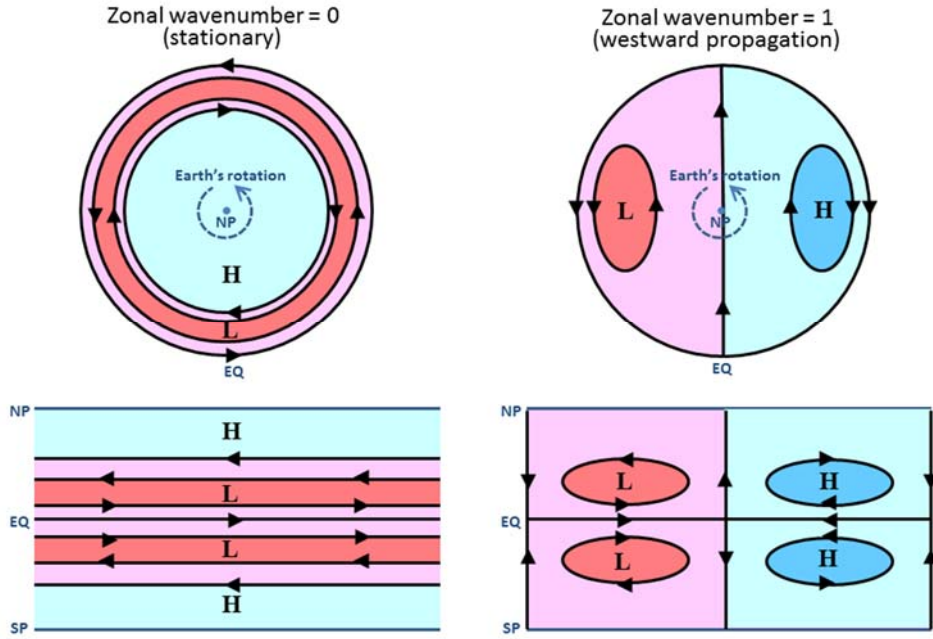
Fig. 5.5 Polar and equatorial views of pressure and wind patterns for Rossby (planetary) waves of $n = 1$ and zonal wavenumber $k \cdot 2\pi a = 0$ (see Shigehisa, 1983, for derivation) and 1 (same as in Fig. 5.1).
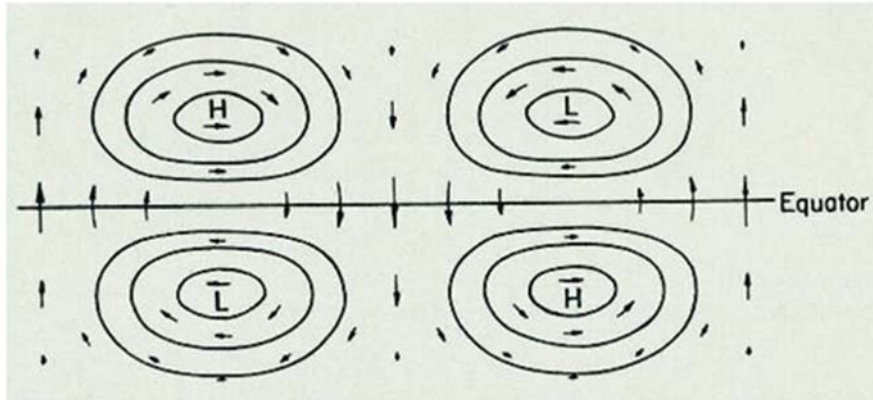

Fig. 5.6 Theoretical horizontal pressure and wind distributions of mixed Rossby-gravity wave (Matsuno, 1966).

a Gaussian-like meridional profile centered at the equator) appropriate roots are only two[43]:

$$\hat{\omega} = \frac{k\beta\lambda^2}{2}\left(1 - \sqrt{1 + \frac{4}{k^2\lambda^2}}\right) = \frac{kN}{(m^2 + 1/4H^2)^{1/2}}\left(\frac{1}{2} - \sqrt{\frac{1}{4} + \frac{\beta(m^2 + 1/4H^2)^{1/2}}{k^2N}}\right) \quad (< 0), \quad (5.18)$$

and the other one (a positive $\hat{\omega}$) similar to (5.18) with a positive sign replacing the negative sign in the bracket (in front of the root) which is an eastward propagating inertio-gravity wave. The westward propagating wave given by (5.18) becomes similar to Rossby wave in the short zonal wavelength limit ($k \to \infty$), and also to inertio-gravity wave in the long wave limit ($k \to 0$). Therefore this wave with $n = 0$ and negative $\hat{\omega}$ is called by Matsuno (1966) as the *mixed Rossby-gravity wave* (Fig. 5.6), or named after the observational discover(s) (Yanai and Maruyama, 1966) as *Yanai (-Maruyama) wave* (see Section 5.4).

All the waves mentioned above are derived from the reduced equation (5.10) only for $\tilde{v}$, and any other waves

---

[43]The other solution $\hat{\omega} = -k\beta\lambda^2 = -kN(m^2 + 1/4H^2)^{-1/2}$ is invalid for the polarization relations (5.10).
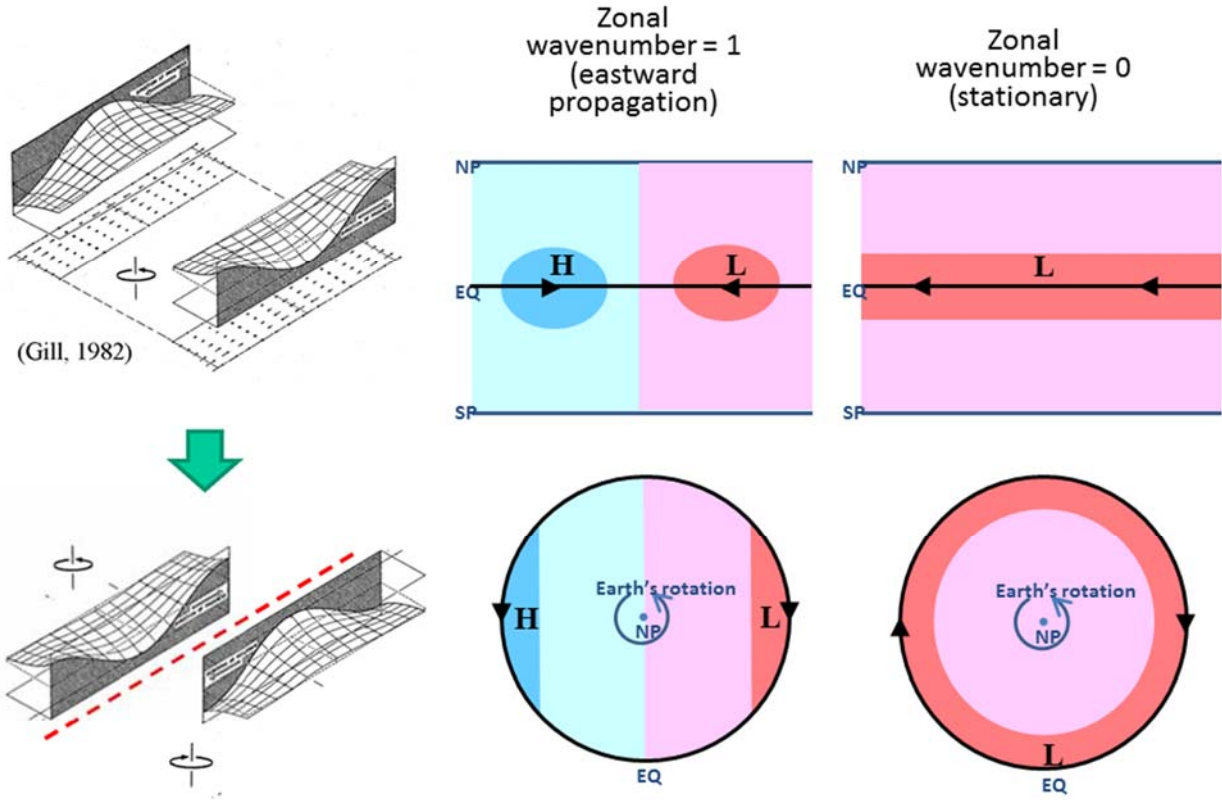
Fig. 5.7 Coastal (left) and equatorial (middle and right) Kelvin waves: the coastal cases for the both hemispheres are combined in the equatorial case just like the equator as a cost (Gill, 1982). For the equatorial Kelvin waves, equatorial and polar views of pressure and wind patterns for zonal wavenumber $k \cdot 2\pi a = 0$ (see Shigehisa, 1983, for derivation) and 1 are shown.

with $\tilde{v} \equiv 0$ (if exist) may not have been included. Matsuno (1966) noticed it, and obtained an additional category of wave satisfying

$$\widehat{\omega} = \frac{kN}{(m^2 + 1/4H^2)^{1/2}}; \quad \frac{\widehat{\omega}}{k}\tilde{u} = \tilde{\phi} \propto e^{-y^2/2\lambda^2}, \tag{5.19}$$

by restarting from the original equation system (5.1), (5.2) and (5.7) with putting $\tilde{v} \equiv 0$[44]. Such an additional solution is expected also from the mathematical completeness of orthonormality of the Hermite polynomials, and is labeled by $n = -1$ which is satisfying (5.14). The dispersion relation in (5.19) is non-inertial gravity-wavelike, but includes only one root propagating eastward ($\hat{c} = \widehat{\omega}/k = \sqrt{gh} > 0$). The meridional profiles of $\tilde{u}$ and $\tilde{\phi}$ are like a Gaussian function centered on the equator with e-folding width $\sqrt{2}\lambda = \sqrt{2\hat{c}/\beta}$. The polarization relation is obtained as $\tilde{u} \approx -(l/k)\tilde{v} \approx -i(l/\beta y)\tilde{\phi}$, which is just geostrophic and completely different from gravity waves. These features are mathematically common to so-called Kelvin waves propagating over the ocean surface along a coastline (always seeing it in the right/left-hand side in the northern/southern hemisphere), and the wave given by (5.19) is called the *equatorial Kelvin wave* (Fig. 5.7). Namely, the equator with changing sign of the Coriolis parameter plays a role of coast trapping this special mode in the both sides. In the lower stratosphere the most dominant modes with zonal wavenumbers 1 or 2 in the equatorial circumference (i.e., zonal wavelengths of 40,000 or 20,000 km; see Section 5.4) have been called also as the *Wallace-Kousky waves* after their discoverers (Wallace

---

[44]The other root $\widehat{\omega} = -kN(m^2 + 1/4H^2)^{-1/2}$ leading an inappropriate result $|\tilde{\phi}| \to \infty$ for $|y| \to \infty$ is omitted from solutions.

and Kousky, 1968), and in the upper stratosphere and mesosphere the period is shorter and the vertical wavelength is longer (Hirota, 1978). In the troposphere the equatorial parts of the most dominant intraseasonal variations (Madden and Julian, 1971; see Section 6.4) are constructed by equatorial Kelvin waves with periods and zonal wavelengths of some tens of days and some thousands of kilometers, and similar or shorter ones are observed also as tropopausal gaps (Shimizu and Tsuda, 1997).

These two special categories, the mixed Rossby-gravity and equatorial Kelvin waves, are collectively called the *equatorial waves*. They have been studied well observationally related to many types of interannual and intraseasonal variations (Sections 5.3−4 and 6.4) which are phenomena not only special for the tropics butt also impactful for the global climate. Advances of high-resolution observation networks and numerical models have contributed the establishment of wave dynamics and its successful applications to understand those phenomena. An important concept of the wave dynamics is *group velocity* given generally by

$$\overline{\boldsymbol{u}} + \frac{\partial \widehat{\omega}}{\partial \boldsymbol{k}}, \tag{5.20}$$

which is introduced as a progression velocity of the whole *wave packet* localized spatially and spectrally, and gives that of wave energy and momentum (exactly speaking, wave action). If we observe wave parameters and determine their types (dispersion and polarization relations), we may understand/predict their progressions/impacts by calculating the group velocity (5.20).

Since 1990s more several times of intense tropo-stratospheric observations mainly over Indo-Pacific regions around the maritime continent by radiosondes and/or wind profilers have revealed that waves with periods longer than a few days observed mainly in the zonal wind ($|u'| \gg |v'|$) are due to eastward propagating equatorial Kelvin waves mentioned above, whereas waves shorter than a few days usually with elliptic polarizations ($|u'| \sim |v'|$) are mainly westward-propagating mixed Rossby-gravity or inertio-gravity waves. These are superposed and organized into a transient localized structure, which appears as so-called hierarchical structure of a (super) cloud cluster (Section 6.4).

5.2. Zonal-vertical (Walker) circulation

The actual tropical diabatic heating is quite different from zonal symmetry, due to land-sea contrast and variations also on land (by topography, physiography, vegetation, etc.) and on sea (mainly by wind-driven currents), and the circulation is also different from the zonal-mean Hadley circulation. In particular, the land distribution of African and American continents and the Indonesian maritime continent (Section 4.4) and weak geostrophic balance in the vicinity of the equator (cf. Section 4.2) may induce a steady zonal circulation, in addition to the meridional Hadley circulation and seasonally reversing monsoons. For example, westward pressure gradient force between relatively low surface pressure over the maritime continent and high surface pressure in the central Pacific drives stronger easterly trade wind in the equatorial western Pacific. This strong wind makes the warm ocean-surface water thicker in the western side, as well as poleward Ekman transport and resulting so-called *equatorial upwelling* of the cold deep water over the central-to-eastern equatorial Pacific. Over the sea surface the easterly transports water vapor more westward, and enhance the upward motion (convective cloud activity) over the maritime continent, which feeds back to the westward pressure gradient and easterly. Therefore a steady circulation is generated between the maritime
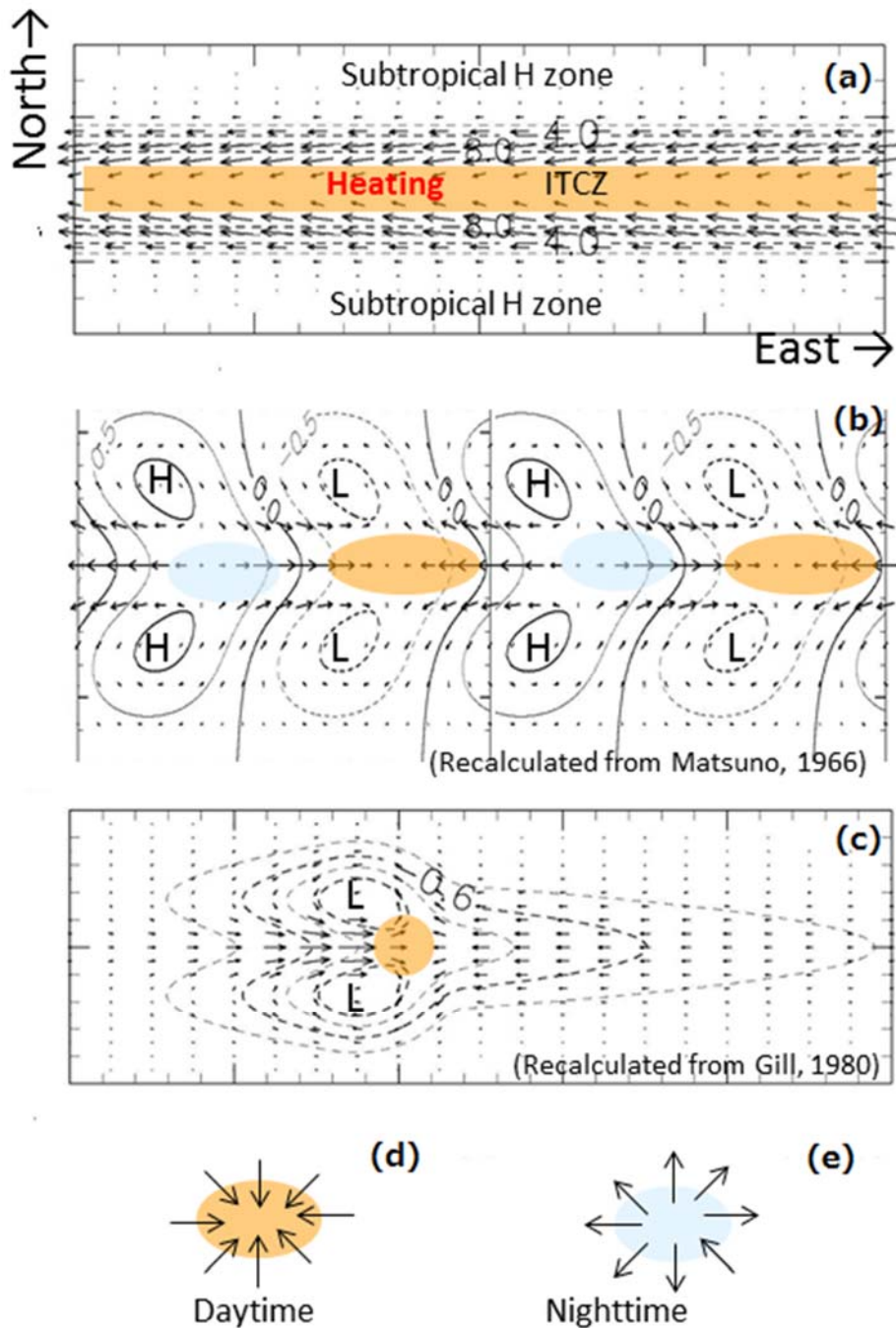
Fig. 5.8 Equatorially forced motions. (a) zonally homogeneous Hadley circulation-ITCZ-trade wind system (Section 4.3) obtained independently from Kosaka and Matsuda, 2005); (b)−(c) Matsuno (1966) - Gill (1980) patterns (see text), corresponding to real and maritime continents, and intraseasonal variations (Section 6.4); (d)−(e) diurnal-cycles sea-land breeze circulations (Section 6.1).

continent and the Pacific, which was called the *Walker circulation* by Bjerknes (1969), "since it can be shown to be an important part of the mechanism of Walker's "Southern Oscillation"" (cf. Section 5.3). Sir Gilbert Walker published many papers on interannual variations of the world climate including monsoons during his 20-year stay in the British Indian Meteorological Department, but he himself did show mainly pressure patterns and not the zonal circulation itself.

Exactly speaking, as discussed in Section 4.3, the distribution of heating/cooling throughout the troposphere is necessary to calculate any circulation, but the essential features of almost steady equatorial circulations may be

explained mainly by the boundary layer situations, of which mainly evaporation and moisture convergence maintain a convective system. Although those are a result of various interactions in the boundary layer and in Earth's surface, we may consider an external diabatic heating for the simplest problem. Furthermore we may assume that the steadiness is maintained by turbulent drag, such as the Rayleigh damping (4.12) and the Newtonian cooling (3.6). Then we replace $\partial/\partial t$ or $-i\omega$ in the wave equations in Section 5.1 with a simple drag coefficient $\alpha\ (>0)$[45], and omit the mean flow $\overline{u}$ for simplicity. Thus (5.10) is modified as

$$\frac{d^2\tilde{v}}{dy^2}+\left[-\left(m^2+\frac{1}{4H^2}\right)\frac{\alpha^2+\beta^2 y^2}{N^2}-k^2+\frac{ik\beta}{\alpha}\right]\tilde{v}=-\tilde{Q}.$$

We may substitute expansions of $\tilde{v}$ and $\tilde{Q}$ by the orthonormal function series $H_n(y/\lambda)$, and obtain the factors of $\tilde{v}_n$ from those of $\tilde{Q}_n$ given arbitrarily. Note that above equation does not involve the (most important) Kelvin wave component ($n=-1$), which must be determined from similar expansions for the polarization relationships.

Matsuno (1966) and Gill (1980) calculated such circulations induced by steady heat sources Q aligned and isolated on the equator, respectively (Fig. 5.8). Gill modeled the *Indonesian maritime continent*[46] on infinitely broad Earth. Matsuno's cyclic specification corresponds to the case of neighboring continents affecting each other, or one continent on spherical Earth. Both obtained basically same results: the so-called *Matsuno-Gill pattern* with Kelvin-wavelike zonal wind along the equator and twin Rossby-wavelike vortices in the both subtropics. Around a heating source (convergence) a zonal ridge with westerly and a trough with easterly appear in the west and east, respectively, and twin cyclonic vortices in the both northern and southern sides of the westerly ridge. Matsuno's results involved also cooling (divergence), around which all the features are completely symmetric to those around the heating. Results around Gill's isolated heating source are zonally not symmetric; the eastern-side easterly is about three times broader longitudinally than the western-side westerly, and the latter is about three times stronger than the former (which is actually observed as a westerly burst). Gill speculated that circulations in the meridional and zonal cross-sections around the heat source correspond to those observed as the Hadley and Walker circulations (Fig. 5.9).

The same calculation may be applied also for an extreme (zonally homogeneous) case $k\to 0$, by which the Hadley circulation is obtained for an equatorially symmetric heating (Fig. 5.8(a); Kosaka and Matsuda, 2005). At the equator the horizontal wind vanishes, because the zero zonal wavenumber modes of Kelvin and Rossby waves (easterly and westerly) are canceled each other. In the both sides of this (the northern and southern subtropics) at the bottom the both waves have easterlies and the Rossby component makes weak equatorward flows (the Hadley cells) just observed as the trade winds in the actual tropical lower atmosphere. These features can be understood (as described by Gill) as the zonally elongated extremity of the Matsuno-Gill pattern.

The vertical structure of the Kelvin waves ($\hat{\omega}>0$) near the equator is expected inclined eastward ($k/m<0$), because the vertical group velocity (5.20) (without vertical mean flow)

$$W\equiv\frac{\partial\hat{\omega}}{\partial m}=-\frac{m\hat{\omega}}{m^2+1/4H^2}\approx-\frac{\hat{\omega}}{m}\quad\text{(opposite to phase velocity)}^{47}\tag{5.21}$$

must be positive, that is, $m<0$. However, the dispersion relation (5.19) implies $|m|\propto N$, which is very small

---

[45]More correctly describing, the time derivative and the wave frequency are deleted ($\partial/\partial t=0$, $\omega=0$), and then the inhomogeneous (external forcing) terms are added as $(G_x{}',\ G_x{}',\ Q')\to-\alpha\,(u',\ v',\ \phi')+(0,0,\ Q)$.

[46]Ramage (1968) first called so, mainly based on thunderstorm frequency distribution (only covering the whole equatorial circumference at that time) with a striking peak in this region, comparable to the other peaks in real continents of Africa and South America.

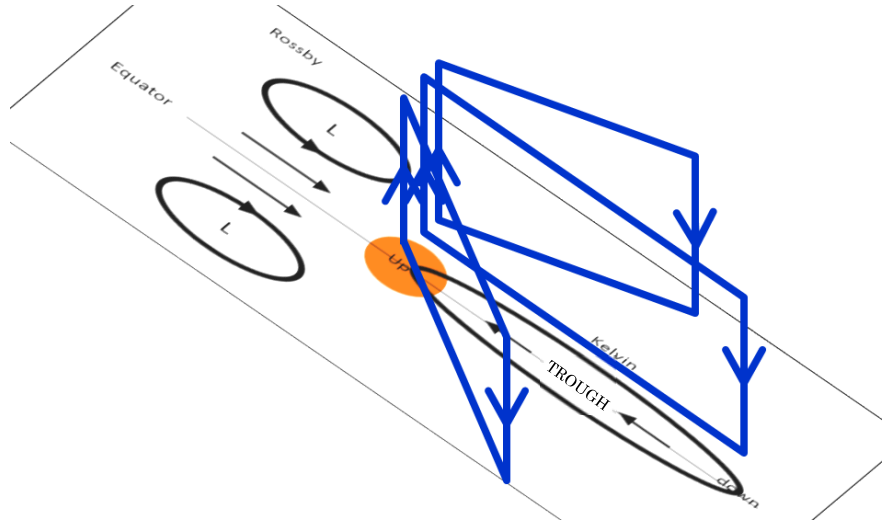[47]This feature is common to the gravity waves.

Fig. 5.9 The Hadley and Walker circulations associated with the Matsuno-Gill pattern.
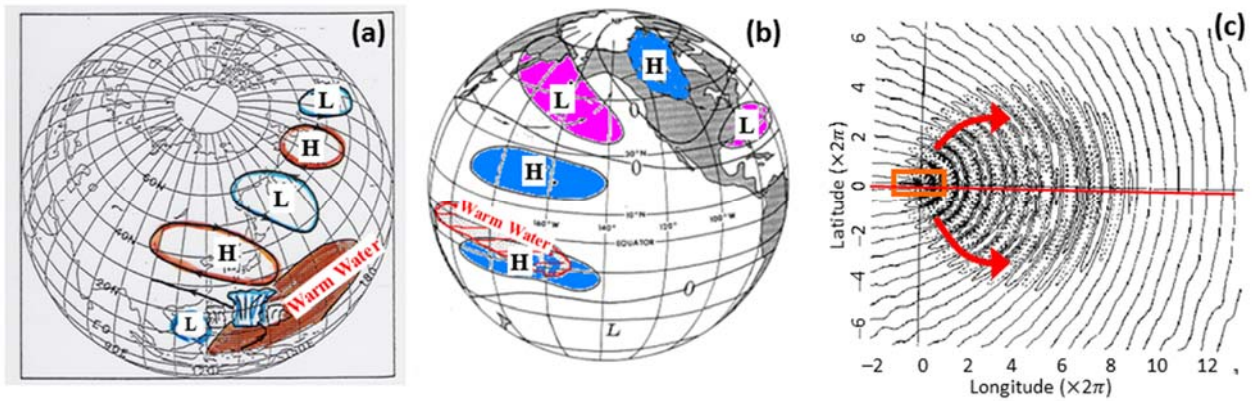

Fig. 5.10 (a) The Pacific-Japan (PJ) (Nitta, 1986) and (b) Pacific-North America (PNA) (Horel and Wallace, 1981) teleconnection patterns, and (c) a shallow-water Rossby wave propagation along a great circle (Hayashi, 1987).

(replacing θ by the equivalent potential temperature defined for moist atmosphere in Section 6.2; in particular $N = 0$ inside a cloud) in the tropical troposphere. Actually observed/analyzed Walker circulation cell has an almost vertical structure.

In summary the tropical circulation between intraseasonal and interannual scales is a superposition of the Hadley, Walker and monsoon circulations. By the Helmholtz theorem (Fug. 4.9 in Section 4.2) such a large-scale circulation may be separated into a non-divergent flow described by the streamfunction ψ and a irrotational field described by the velocity potential χ:

$$u = -\frac{\partial \psi}{\partial y} + \frac{\partial \chi}{\partial x}, \qquad v = \frac{\partial \psi}{\partial x} + \frac{\partial \chi}{\partial y}. \tag{5.22}$$

Taking the horizontal divergence from (5.22) to omit the geostrophic component ($\psi \sim \phi$, of which the zonal mean gives $\overline{u}$):

$$\frac{\partial u}{\partial x} + \frac{\partial v}{\partial y} = \frac{\partial^2 \chi}{\partial x^2} + \frac{\partial^2 \chi}{\partial y^2}, \tag{5.23}$$

we may obtain the potential flow perpendicular to contours of χ, which involves the Hadley, Walker and monsoon circulations (e.g., Krishnamurti, 1971; Krishnamurti et al., 1973; see Figs. 4.14 (a) and (b)). In the northern winter

the northern-hemispheric Hadley cell is reinforced by the 'astronomical' monsoon (Section 4.4), and in the lower troposphere they and the Walker circulation are all flown into the southern-hemispheric side of the maritime continent to make very active rainy season and upper-tropospheric divergence there. In the northern summer the Walker circulation centered at the Indonesian maritime continent has the same direction as a part of the summer 'geographical' monsoon centered at the Tibetan plateau, as well as the southern-Hadley cell reinforced by the 'astronomical' monsoon, and very strong divergence appears in the Tibetan upper troposphere.

The twin cells generated in the both subtropical sides of the Matsuno-Gill pattern are due to Rossby waves which are trapped modes near the equator by the given boundary condition. If we abandon this condition, there are other modes of Rossby waves propagating globally along any great circles (Hoskins and Karoly, 1981; Simmons et al., 1983; Hayashi and Matsuno, 1984), which transfer signals of tropical climate anomalies (Fig. 5.10). The so-called *teleconnection* between climates of distant places were considered long ago by Walker and Bliss (1923, and many others) and then by Bjerknes (1969), and now is explained dynamically by the Rossby wave propagations. Through this mechanism tropically excited phenomena cause abnormal weather and climate all over the world (see the next section).

5.3. Atmosphere-ocean interaction: El Nino-southern oscillation (ENSO) and Indian-Ocean dipole mode (IOD)

As mentioned in the previous section, the Walker circulation (in the same direction as the trade wind) pushes warm surface Pacific water westward, which causes so-called *coastal upwelling* off the South America centered around Peru. Mainly this. as well as cold equatorward currents along coasts of the Americas, keeps quite appropriate (relatively cold) environment for planktons and fishes eating them, namely very good fishery sea area, usually from March to December. From December the westerly monsoon from the Indian Ocean to the maritime continent becomes much stronger than the Pacific trade wind, and relatively weakened coastal upwelling and cold currents make off-Peru water warmer and fishery taking a break. This had been called El Niño (meaning a boy baby) originally (at latest since early Spanish colonial era some hundreds years ago; phenomena themselves probably known since the Inca Empire era), because all godly Peruvian fishermen celebrated Christmas (the birthday of the Holy Baby Jesus). This 'original usual El Niño' recovers at latest until March, associated with the withdrawal of southern Indonesian rainy season. However, every few years, extremely warmer sea water and several abnormal weather such as torrential rainfalls come to this area rather earlier than December and continues often for a year. Because the cause is different (as described below) from the usual one, the abnormal one was distinguished initially and called El Niño-like phenomenon etc., but now only this abnormal one (and often including related abnormal weather) is called *El Niño*.

Independently, from studies on interannual variations of monsoon and correlated phenomena at the Indian Meteorological Department, the Director General Walker (1923) discovered the so-called *southern oscillation* that surface pressure anomalies (from each long-duration means) at Darwin of Australia and Tahiti Island of the central Pacific have clear variations correlated negatively with each other at 2–5 year intervals. Almost half a century later, Bjerknes (1969) speculated the existence of so-called Walker circulation varying with the Darwin-Tahiti (and the whole Indo-Pacific) pressure anomalies, and all of them are related to El Niño (and opposite phase). In the eastern Pacific during the weaker Walker-circulation trade wind phase of the southern oscillation, the equatorial and coastal oceanic upwellings are reduced, the thermocline is deepened, and the sea surface temperature rises, that is referred
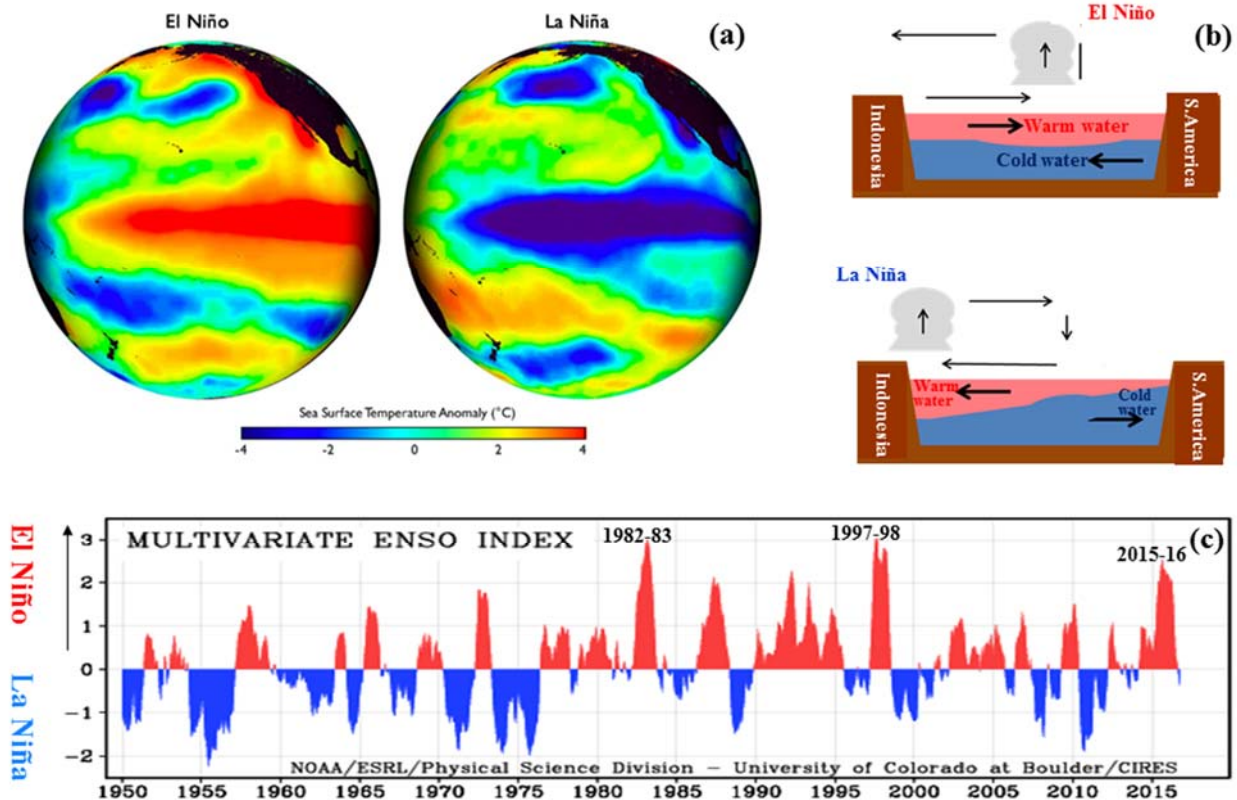
Fig. 5.11 El Niño and La Niña: (a) typical sea surface temperature distributions (Fiondella, 2009), (b) schematic zonal cross-sections of the equatorial Pacific and (c) 65-year variation of an index (http://www.esrl.noaa.gov/psd/enso/mei/).

to as El Niño. In the opposite phase, stronger trade wind induces stronger upwelling, shallower thermocline and cooler sea surface temperature in the eastern equatorial Pacific, whereas deeper thermocline and warmer surface water in the western Pacific and inland/surrounding seas of the maritime continent, that is (initially called the anti-El Niño but now taking another Spanish word on a girl baby) *La Niña*. The whole cycle of these events is called the *El Niño-southern oscillation (ENSO)*.

ENSO is, exactly speaking, not an 'oscillation' but is rather irregular interannual variation as the intervals (not 'periods') are changed in the range of 2-5 years (Fig. 5.11). It is like a global scale "see-saw" in atmospheric pressure and in the ocean thermocline[48]. The both phases El Niño and La Niña are the two 'stable' situations of this sea-saw, and must not be considered that one is normal and the other is abnormal. ENSO is a typically atmosphere-ocean coupled (interacting) phenomenon, and must not be considered which of atmosphere or ocean is the cause or the result. Anyway, associated with ENSO, the regional (the maritime continent, the Pacific, and the South America) climates such as rainfall and temperature are varying interannually (as seen only partly already in Fig. 4.17). Furthermore, the atmospheric anomalies may be propagated globally by (Rossby) waves, as shown later. Therefore, ENSO is one of the key issue to understand and predict interannual (a few-year scale) climate variability all over the world, and this is one of the major reasons why the tropical meteorology/climatology becomes a hot study subject.

In order to study this atmosphere-ocean coupled phenomenon, we may use (5.1), (5.2) and (5.7) for the

---

[48]Intervals of the South America, Africa and maritime continents (where the atmospheric updraft-convection centers are located in the La Niña phase) are roughly a quarter of the equatorial circumference. The central Pacific and the two true continents (updraft-convection in El Niño) have also similar intervals. In this meaning ENSO is alternative forced modes of zonal wavenumber four.

atmospheric process, and add another similar equation system for the oceanic process. At first, let us sketch the simplest steady solution of this six-variable six-equation system. For the atmosphere, on one hand, we assume a (latent and/or sensible) heating source $Q'_{(atmosphere)}$ dependent on the oceanic surface temperature, and neglect mechanical forcing ($G'_{x(atmosphere)} = G'_{y(atmosphere)} = 0$) for simplicity. The steady atmospheric response is the Matsuno-Gill pattern obtained so far in the previous section. For the ocean, on the other hand, we neglect heating ($Q'_{(ocean)} = 0$), and assume a mechanical forcing $\left(G'_{x(ocean)},\ G'_{y(ocean)}\right) \equiv +\alpha'\left(u'_{(atmosphere)}, v'_{(atmosphere)}\right)$ due to wind stress[49]. We also assume that the final steady ocean situation is adjusted as a completely flat ocean surface ($h' \to 0$), and we have

$$u'_{(ocean)} \approx \frac{G_y{}'_{(ocean)}}{\beta y} = \frac{\alpha'}{\beta y} \cdot v'_{(atmosphere)},$$

$$v'_{(ocean)} \approx -\frac{G_x{}'_{(ocean)}}{\beta y} = -\frac{\alpha'}{\beta y} \cdot u'_{(atmosphere)},$$

(5.24)

which is similar to the meridional flow in the steady forced meridional circulation (4.20). (5.24) shows the sea water moves to the right-/left-hand side of wind targeting direction in the northern/southern hemisphere ($y > 0$ / $y < 0$).[50]

In the La Niña phase with convection center over the maritime continent, there are generated twin anticyclones in the northern and southern sides of a divergence over the central equatorial Pacific (as calculated by Matsuno), which intensify the both subtropical high pressure zones and a convergence ($v'_{(atmosphere)} \lessgtr 0$ for $y \gtrless 0$) at the equator off the South American coast, whereas the ocean water is transported westward ($u'_{(ocean)} < 0$) for the both hemispheres as in (5.24) and, to compensate it, the coastal upwelling is generated. Near the equator, due to intensified trade wind ($u'_{(atmosphere)} < 0$) transports the ocean water poleward ($v'_{(ocean)} \gtrless 0$ for $y \gtrless 0$), which is compensated by the equatorial upwelling. By these processes relatively cooler water region is elongated from the South American coast westward along the equator, and the surface warm water is transported and accumulated (as so-called *warm water pool*) in the western end of the Pacific. Therefore these processes feed back to maintain the Matsuno-Gill pattern for La Niña stably.

In the El Niño phase with convection center over the central Pacific, the Matsuno-Gill pattern in the opposite sense to the La Niña phase is maintained similarly. Therefore the both La Niña and El Niño situations may be maintained stably as steady solutions. If we want to study transience between La Niña and El Niño, we need to solve time-dependent equations with nonlinearity and dissipation. Even in this case we may assume that the atmosphere respond quickly to the sea surface temperature through $Q'_{(atmosphere)}$, and generate a Matsuno-Gill pattern. We may solve the time-dependent nonlinear dissipative oceanic equations for $\left(G'_{x(ocean)},\ G'_{y(ocean)}\right)$ given by the

---

[49]Because the forcing by wind for ocean is the counteraction of the forcing (friction) by ocean for wind, the sign becomes opposite between atmosphere and ocean. Note that the friction is neglected in comparison with heating in the atmospheric equations (and heating is neglected in the oceanic equations).

[50]More exactly speaking, the forcing $\left(G'_{x(ocean)},\ G'_{y(ocean)}\right)$ is the internal friction (stress gradient) dependent on the depth in the oceanic boundary layer, and its boundary value at the surface is given by the wind stress as in (5.24). Then the exact steady solution for the vertical profile (hodograph) of ocean current $\left(u'_{(ocean)}, v'_{(ocean)}\right)$ throughout the boundary layer is the so-called *Ekman spiral*, and its surface direction is 45° of the right-/left-hand side of wind. Even in this case the mass transport throughout the so-called *Ekman layer* is just as in (5.24) (which is used in Fig. 4.18). The atmospheric Ekman layer (which appears only when the Coriolis parameter is sufficiently large away from the equator) is briefly mentioned in Section 6.3.

atmospheric Matsuno-Gill Pattern. The direct integration of such equations can be done only numerically, and operational prediction results by world's various institutions are obtained for example at a website belonging to Columbia University of US: http://iri.columbia.edu/our-expertise/climate/forecasts/enso/current/ as well as that of each original institution. For semi-analytical or theoretical studies, some simplified equations to predict temperature changes are proposed, as described below.

A simplified equation to model the oceanic temperature change is

$$\frac{\partial T'}{\partial t} = -au' + bh' - cT'; \qquad a, b, c > 0, \tag{5.25}$$

where the three terms in the righthand side are the zonal advection (a: zonal temperature gradient), the warming due to deepening h' of the surface layer, and the dissipation expressed by the Newtonian cooling. From (5.25) T' determines $Q' \approx +\alpha'T'$, for which the atmospheric Matsuno-Gill response is calculated to determine oceanic u' and h'. 'Slow' variations of u' and h' are due to oceanic Kelvin and Rossby waves, which are neutral (not developed) solutions of the oceanic equations. However, Philander et al. (1982) showed that, coupled with the atmosphere, they may be unstable and self-developed. When the last two terms of (5.25) are dominant: $h' \approx (c/b)T'$, an ocean warm anomaly ($T' > 0$) makes atmospheric heating ($Q' > 0$) to generate (Matsuno-Gill pattern-like) atmospheric convergence, which makes oceanic forcing G' to generate oceanic (Kelvin wave and) convergence. In this case the oceanic (Kelvin wavelike) eastward current and the atmospheric (Rossby twin vortices') westerly are in the same direction, and the coupled warm water-active convection (cloud) system is developed rapidly. If this coupling development mechanism works actually, the wind convergence of atmosphere with small inertia must be sustained long enough to keep a positive correlation to induce the current convergence of ocean with large inertia. Key processes are small-scale dynamics and thermodynamics in the ocean surface layer to respond atmospheric forcing, and oceanic waves to extend local variations for broader area. In the latter process each equatorial wave is restricted in the propagation direction, and the oceanic waves cannot propagate beyond coasts.

It is possible that a wave is reflected as another type of wave. For example westward propagating Rossby wave reaching at the western coast is reflected as eastward propagating Kelvin wave. When a coupled 'warm' anomaly propagates eastward, an opposite (cold) anomaly will be emitted as a Rossby wave, which is reflected as an again reversed (warm, the same as the original) anomaly as a Kelvin wave. To express these processes, the third term of (5.25) is separated into a response directly dependent on $T'(t)$ and another one $T'(t - \tau)$ due to wave round-tripped for a time delay τ. The second term of (5.25) is expressed by a linear term dependent on T' and (when h' is amplified) nonlinear term dependent on T'^3. The first (advection) term is mainly dependent on T'. Therefore a revised equation may be written as

$$\frac{\partial T'}{\partial t} = -b'T'(t - \tau) + c'_1 T' - c'_2 T'^3; \qquad b > c'_1 > 0, \qquad c'_2 > 0, \tag{5.26}$$

which resembles a 'delayed oscillator' (Battisti and Hilst, 1989). If a steady state appears after a sufficiently long time ($t \gg \tau$, $\partial/\partial t \approx 0$), (5.26) gives (a trivial solution $T' \approx 0$ and) a pair of solution:

$$T' \approx \pm\sqrt{(c'_1 - b')/c'_2}, \equiv \pm T_0,$$

corresponding to La Niña and El Niño. Substituting a perturbation to the steady solution: $T' - T_0 \equiv \epsilon e^{-i\omega t}$ into (5.26) and taking the imaginary part of terms of the order of ϵ, we obtain $\omega \approx b' \sin \omega\tau$, from which we may study

the stability.

The tropically excited climate anomalies such as ENSO may affect globally by the Rossby wave-teleconnection mechanism mentioned in the end of previous section. An often observed teleconnection is the *Pacific-North America (PNA) pattern* in northern winter transferring El Niño-induced anomalies and causing abnormal weather over US (Horel and Wallace, 1981). Another one is the *Pacific-Japan (PJ) pattern* in northern summer (Nitta, 1986) and in northern winter (Chen, 2002). On the contrary extratropical situations may affect and interact with the tropical phenomena by similar mechanisms. For example, interannual anomalies of pressure (and so-called polar vortex under the geostrophic balance) in the northern high latitudes (called the *arctic oscillation (AO)*; Thompson and Wallace, 1998) may propagate equatorward, and modify the ENSO effects in the mid latitudes.

As mentioned in the previous section, the northern summer monsoon forced by the Tibetan plateau is considered to be connected with the Walker circulation, and hence also directly or indirectly with ENSO (e.g., Lukas et al., 1996; Webster et al., 1998). As the discovery of the southern oscillation by Walker (1923), ENSO is interacted directly with and the onset, activity and withdrawal of monsoons, and many studies are still in progress. Indirect connections are through the Indonesian throughflow from the Pacific to the Indian Ocean (e.g., Gordon, 2005), which is an important part of the global ocean circulation (see Fig. 4.8) and is known to be varied sensitively with wind variations such as monsoons and intraseasonal variations (Section 6.4).

Observations of ENSO with sufficient coverage and reliability have been continued from 1950s. Definitions of El Niño and La Niña are slightly different between countries (national operational agencies), institutions and investigators, and details are out of the scope of this mainly theoretical textbook. According to Japan Meteorological Agency (http://ds.data.jma.go.jp/tcc/tcc/products/elnino/index.html), El Niño periods occurred in 1951/52, 1953, 1957/58, 1963/64, 1965/66, 1968−70, 1972/73, 1976/77, 1982/83, 1986/88, 1991/92, 1997/98, 2002/03, 2009/10 and 2014−16, and among them the three biggest events were 1982/83, 1997/98 and 2014−16. La Niña periods occurred in 1949/50, 1954−56, 1964/65, 1967/68, 1970−72, 1973/74, 1975/76, 1984/85, 1988/89, 1995/96, 1998−2000, 2005/06, 2007/08 and 2010/11 (see Fig. 5.11(c)). Remarkable varieties of events have been suggested, for example the *El Niño Modoki*[51], in which the western Pacific resembles El Niño but the eastern not (Ashok et al., 2007).

A phenomenon similar to the Pacific ENSO has been observed as the *Indian Ocean dipole mode (IOD)* (Saji et al., 1999). In the 'positive IOD' phase the sea surface water is anomalously cooling/warming in the eastern/western equatorial Indian Ocean, and in the 'negative IOD' phase everything is opposite. For the western maritime continent rainfall correlations with both ENSO and IOD have seasonality and locality. In the western (Indian Ocean) coast of the middle (equatorial) Sumatera rainfall is correlated with IOD rather than ENSO (Fig. 5.12(b)). The rainy season onset comes later (earlier) in El Niño (La Niña) years than the average at many stations of the southern-hemispheric side (see lower panels of Fig. 4.17; Hamada et al., 2002), and in the northwestern Jawa drought in the dry season (May−October) occurs in conjunction with simultaneous development of positive IOD and El Niño, whereas wet conditions tend to appear in negative IOD with or without La Niña (Fig. 5.12(c); Hamada et al., 2012). Large-scale divergence (convergence) and lower (higher) atmospheric water vapor content tend to suppress (induce) rainfall in northwestern Jawa during the dry seasons of positive (negative) IOD years with cooler (warmer) sea surface temperature. However, such a clear correlation is not seen in the rainy season, and the rainfall amount throughout a

---

[51]'Modoki' is a Japanese word, meaning '…oid', '-like', etc., namely resembling but different.
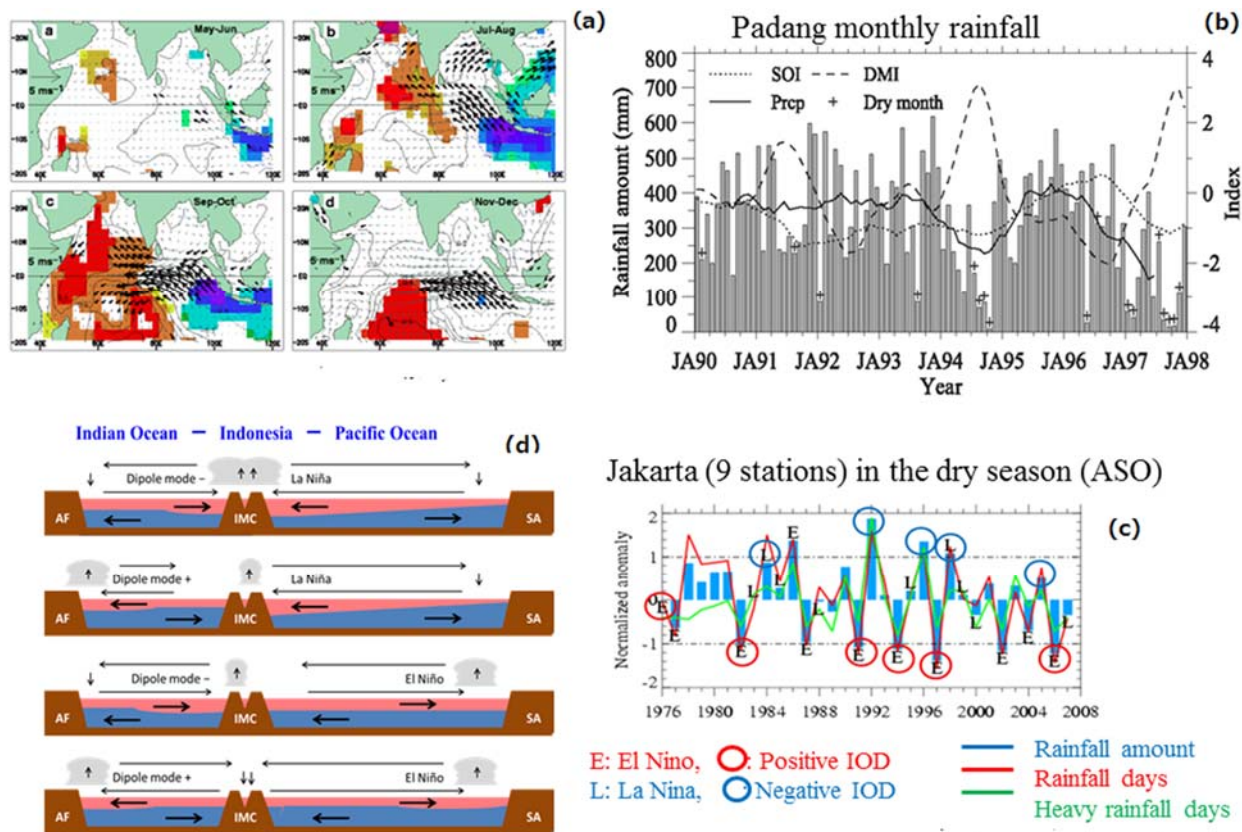
Fig. 5.12 (a) The Indian ocean dipole mode (IOD) (Saji et al., 1999), and its and ENSO's correlations with (b) monthly rainfall in Padang (Hamada et al., 2008) and (c) dry-season (August-October) rainfall in Jakarta (Hamada et al., 2012). (d) Schematic figure of the maritime continent and surrounding oceans with combination of IOD and ENSO (Yamanaka, 2016).

rainy season is not dependent upon the length of the rainy season (between onset and withdrawal) in many areas (Haylock and McBride, 2001; Hamada et al., 2002; McBride et al., 2003). Such low correlations may be due to anomalous Walker circulation patterns on the Indian Ocean side and steep mountains barriers there (Chang et al., 2004a), and due to more direct influence by the cold monsoon surges from the northern mid latitudes (Tangang et al., 2008; Hamada et al., 2012). For the eastern maritime continent (roughly to the east of central Kalimantan mountains) correlations with ENSO are relatively stronger (Aldrian and Susanto, 2003; Kubota et al., 2011; Lestari et al., 2016), due to monsoons as well as direct effects of water temperature of the Pacific.

5.4. Wave-mean flow interaction: Quasi-biennial oscillation (QBO) and semi-annual oscillation (SAO)

The pioneering tropical balloon observations by van Bemmelen (1913) at Batavia (now Jakarta) in the early 20th century noticed already the lower-stratospheric zonal wind variations non-synchronous with the tropospheric seasonal cycle (cf. right top panel of Fig. 3.4). Almost half a century later, Reed et al. (1961) and Veryard and Ebdon (1961) independently discovered that the equatorial lower-stratospheric zonal wind has a *quasi-biennial oscillation (QBO)* with features that successive easterly/westerly regimes appear above 30 km altitude every about 24 to 30 months, propagate downward by about 1 km/month without loss of amplitude, and disappear rapidly below 23 km (Fig. 5.13). This oscillation is zonally symmetric, and also symmetric about the equator with a maximum amplitude of about 20 m/s and a half-width of about 12º. Because of the zonal symmetricity, the mean meridional circulation is very small, and the temperature field satisfy the thermal wind balance (4.11) (or its L'Hospital rule version) with the
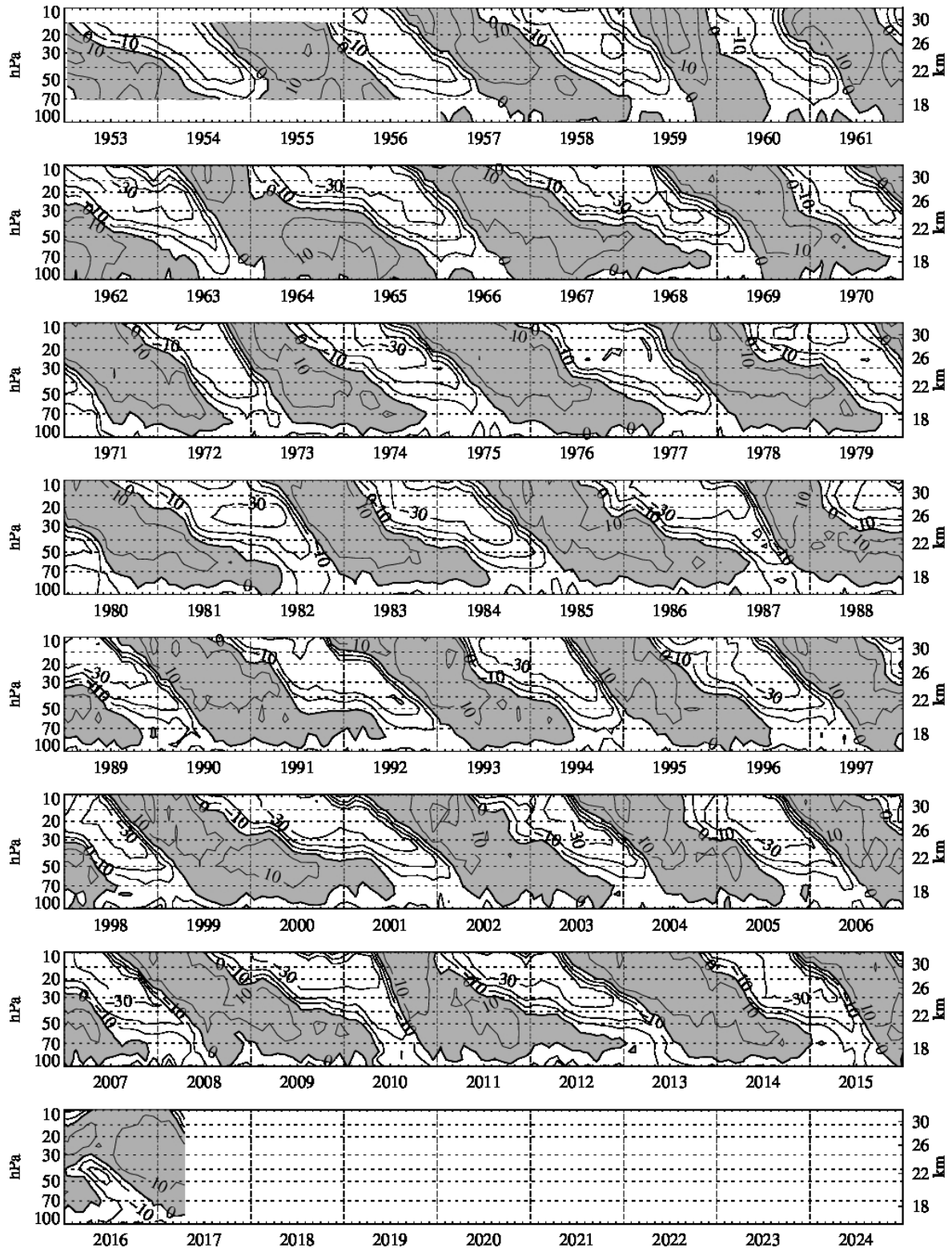
Fig. 5.13 Monthly mean zonal winds (10 m/s intervals; westerlies shaded) at Canton (Jan 1953-Aug 1967), Maledve (Sep 1967-Dec 1975) and Singapore (Jan 1976-). (updated from Naujokat, 1986; http://www.geo.fu-berlin.de/en/met/ag/strat/produkte/qbo/)

zonal wind. From the observed magnitude of vertical shear of the mean zonal wind at the equator is ∼5 m/s/km, the temperature perturbation amplitude over the meridional width ∼1200 km is estimated as ∼3 K. From the L'Hospital version concerning the second derivative of temperature with the opposite sign to the temperature at the equator, the westerly and easterly shear zones have warm and cold equatorial temperature anomalies, respectively.

72

This phenomenon shows periodic behavior not associated with a periodic forcing, and becomes a big problem in atmospheric dynamics. Quantitatively the approximate biennial periodicity and the downward propagation without loss of amplitude must be explained. The occurrence of zonally symmetric westerly (superrotation; cf. Section 4.1) at the equator is also a mystery, and any plausible angular momentum supply and accumulation mechanisms (if due to any wave, what type of wave is sufficiently responsible) must be considered to explain the westerly phase of the oscillation.

The essential explanation was given as the wave-mean flow interaction theory by Lindzen and Holton (1968), Holton and Lindzen (1972), Plumb and McEwan (1978), and others. We start from a simplified version of the mean zonal momentum equation (4.2) or potential vorticity equation (4.27):

$$\frac{\partial \overline{u}}{\partial t} = \frac{1}{\rho_0} \frac{\partial \overline{E}_z}{\partial z} = -\frac{1}{\rho_0} \frac{\partial \rho_0 \overline{u'w'}}{\partial z}, \tag{5.27}$$

in which the righthand-side (gradient of the Reynolds stress; cf. Section 6.1) is now regarded as the divergence of wave momentum flux. As a perturbation theory (asymptotic expansion) $\overline{u}$ in (5.27) should be a second order quantity concerning the wave amplitude[52].

Above equation is identified with the wave action conservation law in the wave mechanics of general physics (Andrews and McIntyre, 1976):

$$\frac{\partial A}{\partial t} = -\frac{\partial B}{\partial z}; \quad A = \frac{E}{\widehat{\omega}}, \quad B = AW, \tag{5.28}$$

where A is the wave action density, B is the vertical wave-action flux, E is the energy density, and W is the vertical group velocity (the vertical component of (5.20); for gravity and Kelvin waves it is (5.21))[53]. kA and kB are called the wave momentum and the wave momentum flux, respectively. Because $kB = \rho_0 \overline{u'w'}$ is obtained from gravity wave solutions (inertio-gravity waves in Section 5.1 at the equator), we may write[54]

$$\frac{\partial}{\partial t}(\rho_0 \overline{u} - kA) = 0. \tag{5.29}$$

From (5.28) we have $kB = kAW = kEW/\widehat{\omega}$, and may calculate A, as well as $kB = \rho_0 \overline{u'w'}$, from wave solutions. It may be shown that A directs to the same direction as $\widehat{\omega}$.

From (5.21) waves with smaller $|\widehat{\omega}|$ have slower group velocity $|W|$ and stay there for longer duration, therefore they are more easily affected by damping such as viscosity and/or Newtonian cooling (even if the simplified equation does not incorporate them explicitly). From the dispersion relation (5.16) waves with smaller $|\widehat{\omega}|$ have larger $|m|$, i.e., shorter vertical wavelengths and larger vertical gradients (shear and/or lapse rate), therefore local instabilities and *wavebreaking* occur more easily. From (5.11), if the horizontal propagation is in the same direction as the mean flow, in particular

$$\text{if} \quad \omega \to \omega\overline{u}, \quad i.e., c \to \overline{u}; \quad \text{then} \quad \widehat{\omega} \to 0, \quad W \to 0 \text{ and } |m| \to \infty \tag{5.30}$$

---

[52]To express this clearly, the mean flow is often written as $\overline{u}^{(2)}$.

[53]The second formula of (5.28) is the same form as the energy of photon in quantum mechanics: $E = h\nu$, where ν is frequency (of electromagnetic wave; see Chapter 1), and h is the Planck constant (with dimension of action). In this meaning (5.28) is often called the *photon analogy*.

[54]It is *not* always that $kA = \rho_0 \overline{u}$, because waves may transmit the media without any interactions (breaking, damping or modulations) and the wave momentum may not be changed to a real momentum of the mean field. In this meaning kA is often called the *pseudomomentum*. (5.29) also implies that c $(= \omega/k)$ may be changed (*self-accelerated*) by nonlinear interactions, if $\overline{u}$ is changed (Fritts and Dunkerton, 1984; Tanaka and Yoshizawa, 1985).
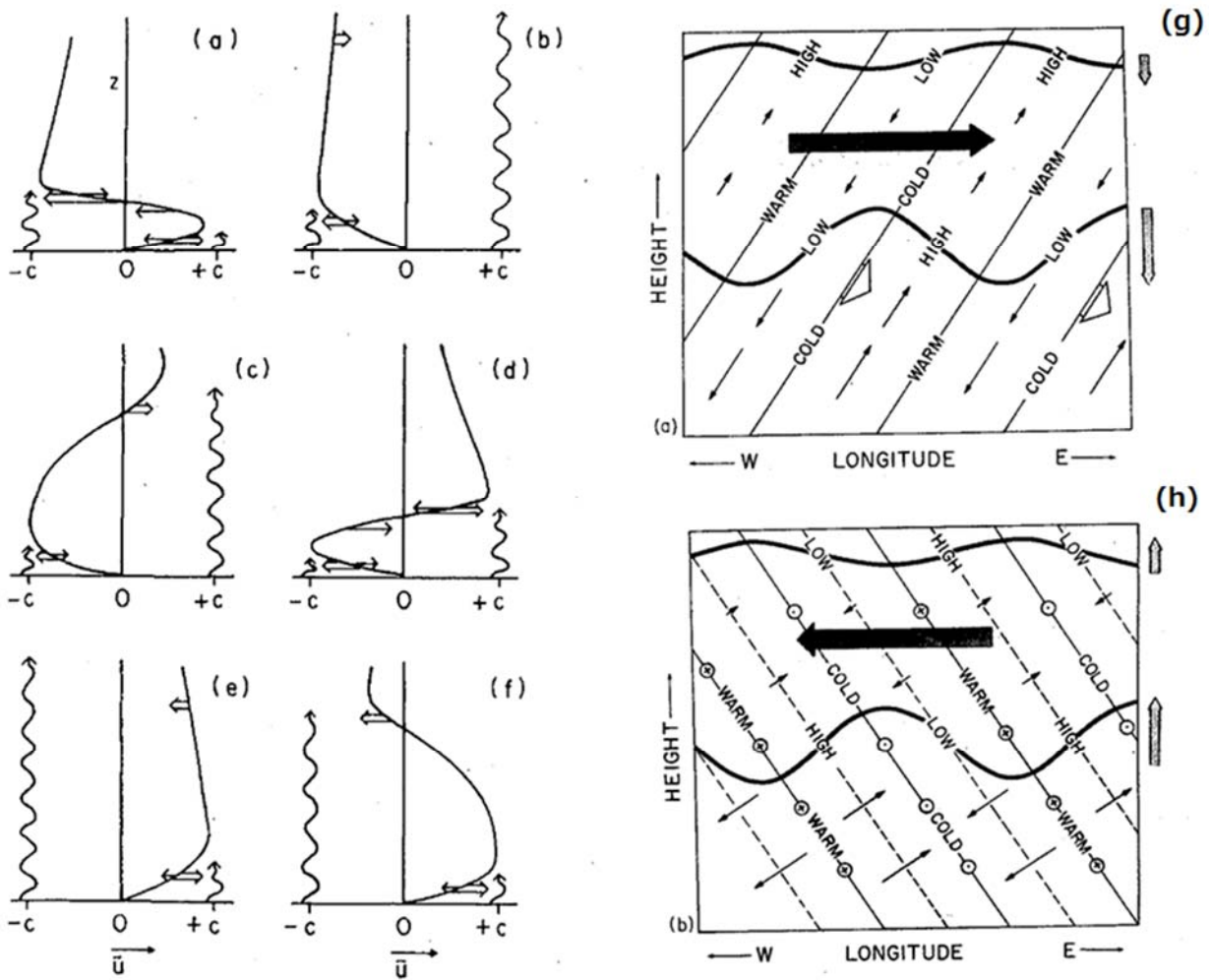
Fig. 5.14 (a)−(f) The QBO-cycle mechanism suggested by the laboratory experiments by Plumb and McEwan (1978): wavy arrows are east- and west-ward waves; double and single straight arrows are wave- and viscosity-driven acceleration (Plumb, 1984). Longitude-height structures of (g) Kelvin along the equator) and (h) mixed Rossby-gravity (along a latitude north of the equator) waves and their latitudinally integrated accelerations (thick horizontal arrows) are also shown (Andrews et al., 1987).

and waves are expected to break. If the media is almost without dissipation and almost homogeneous horizontally, waves conserve ω, k and c; but if there is a mean vertical shear (even weak), there may be the so-called '*critical level*' at which (5.30) is satisfied. Exact theoretical consideration show that (as long as the mean field is stable) gravity waves cannot transmit through the critical level with a significant amplitude and within a finite time, and namely they are substantially absorbed there (Booker and Bretherton, 1967).[55]

For waves propagating horizontally in the direction opposite to the mean flow, there are no such situations. As an earliest study Eliassen and Palm (1961) showed for gravity waves in a non-dissipating atmosphere

$$\frac{\partial}{\partial z}\rho_0\overline{u'w'} = 0 \quad \text{for} \quad \widehat{\omega} \neq 0, \tag{5.31}$$

then (5.27) implies $\partial\overline{u}/\partial t = 0$, that is, there are no change (no acceleration nor deceleration) of the mean flow

---

[55]For the inertio-gravity waves with $f \neq 0$, the critical level is exactly not at $\widehat{\omega} = 0$ but at $|\widehat{\omega}| = |f|$ (Jones, 1967; Yamanaka and Tanaka, 1984). However, in particular in the tropics where $|f|$ is small, the wavebreaking and mean flow interaction will start sufficiently before any effect of f appears.

except at the critical level. This (as well as similar ones for other waves) is called the *non-acceleration theorem*. For example, in the westerly (eastward; $\overline{u} > 0$) the westward waves ($c < 0$) from the bottom propagate upward very quickly and transport the westward momentum ($kA < 0$) to the upper altitudes, whereas the eastward waves ($c > 0$) may encounter their critical levels somewhere and release the eastward momentum ($kA > 0$) there with decreasing the momentum flux ($\partial kB/\partial z < 0$) and accelerating the mean flow ($\partial \overline{u}/\partial t > 0$). During breaking the wave amplitude may be limited so as to keep a marginal state (which is called the wave *saturation*), and we may parameterize the eddy diffusivity K so as to realize a decaying factor $K\partial^2/\partial z^2 \approx -Km^2$ just for keeping the saturation amplitude (Lindzen, 1981). (5.31) also implies amplification of waves to compensate the density decrease, which is more effective (more easily to break) for the waves propagating to the mean flow direction, but is not negligible also for oppositely propagating waves arriving near the top. The last process mentioned above makes the opposite (easterly, i.e., westward) acceleration there.

Once easterly ($\overline{u} < 0$) is generated near the top, it plays a role of critical levels for westward waves ($c < 0$). Then the processes opposite to those mentioned above are started, and continued until the easterly layer arrives at the bottom. Just after the westward waves complete to accelerate the easterly in the lower altitudes, and eastward waves start again the westerly acceleration from the top. The QBO is just repeating these processes (Fig. 5.14). Both observational studies and theoretical models confirmed that energetically upward propagating equatorial Kelvin waves supply westerly momentum (i.e., u' and w' are positively correlated so that $\overline{u'w'} > 0$) probably enough to produce at least major part of the westerly phase of the QBO. However, although the mixed Rossby–gravity waves may provide a significant fraction of the westward momentum necessary to drive the QBO, contribution of mid-latitude Rossby waves and equatorial westward-propagating inertio-gravity waves is inevitably necessary.

Such origins of momenta are closely related to the generation mechanisms of equatorial and other waves maintaining the QBO. Rapid advances of spatially-temporally high-resolution and continuous observations, (e.g., Tsuda et al., 1994a, b, 2000; Sato et al., 1994, 1999; Ogino et al., 1995, 2016), as well as numerical modelling (e.g., Horinouchi and Yoden, 1996; Horinouchi et al., 2002, 2003), revealed clear tropical maximum of stratospheric gravity-wave activity in particular over the Indonesian maritime continent, where the tropospheric convective clouds also take maximum[56]. Momentum flux of such gravity waves have been requested to simulate the stratospheric dynamics such as equatorial quasi-biennial oscillations (Sato et al., 1999; Kawatani et al., 2010a, b). Effects of global warming on the QBO (e.g., Kawatani and Hamilton, 2013) and very recent abnormal behavior of the QBO (e.g., Osprey et al., 2016) are also studied in view of variabilities of related waves.

Above the QBO region, observations in the low latitudes are quite limited, by each small number of satellites (mainly thermal-wind estimations), lidars, VHF radars (above the middle mesosphere), large plastic balloons (below the stratopause) and rocketsondes (until around 2000). In the upper stratosphere-lower mesosphere (35−60 km altitudes) around the stratopause and in the upper mesosphere-lower thermosphere (70−90 km altitudes) around the mesopause, there are semiannual oscillations (SAOs) of anti-phase with each other (Reed, 1965; Hirota, 1978). Their generation mechanisms are considered essentially similar to the QBO, but by faster (longer-vertical wavelength)

---

[56] Because the sea-land circulation as the most dominant mode over the maritime continent is a horizontal convection, that is a superimposition of upward and downward propagating internal gravity waves, they may be modified if the background wind is changed. The diurnal cycle migration of convergence-cloud zone implies also generation of gravity waves of both landward and seaward propagations. See Yamanaka (2016) and Yamanaka et al. (2017).

eastward Kelvin waves (Hirota, 1979) and winter mid-latitude westward Rossby waves (Dunkerton, 1979, 1982), as well as inertio-gravity waves. Probably because these waves are originally from the lower atmosphere, the SAOs are modulated by the QBO and meridional circulations (e.g., Garcia and Sassi, 1999). In the much higher region (90−110 km altitudes) easterlies are dominant throughout a year, which are considered due to effects by diurnal thermal tides generated in the stratospheric ozone layer (Miyahara, 1981). Tides are dominant and important phenomena in the thermosphere including (Kato, 1980). Tides are also generated by water vapor absorption of infrared radiation in the troposphere, and appear as semidiurnal variability of surface atmospheric pressure. The global-vertical structures of diurnal tides are also studied, in particular on their excitation/amplification in the tropics (e.g., Sakazaki et al., 2012).

Exercise 5

Knowing the Matsuno's theoretical solution for equatorial waves:

$$\phi_n = e^{-\frac{1}{2}y^2} H_n(y)$$

$$\begin{pmatrix} v \\ u \\ \phi \end{pmatrix}_{-1} = \begin{pmatrix} 0 \\ \phi_0 \\ \phi_0 \end{pmatrix}$$

$$\begin{pmatrix} v \\ u \\ \phi \end{pmatrix}_{ol} = \begin{pmatrix} 2i(\omega_{ol}+k)\phi_0 \\ \phi_1 \\ \phi_1 \end{pmatrix}$$

$$\begin{pmatrix} v \\ u \\ \phi \end{pmatrix}_{nl} = \begin{pmatrix} i(\omega_{nl}^2 - k^2)\phi_n \\ \frac{1}{2}(\omega_{nl}-k)\phi_{n+1} + n(\omega_{nl}+k)\phi_{n-1} \\ \frac{1}{2}(\omega_{nl}-k)\phi_{n+1} - n(\omega_{nl}+k)\phi_{n-1} \end{pmatrix}$$

and the Hermit polynomials:

$$H_0(\eta) = 1, \quad H_1(\eta) = 2\eta, \quad H_2(\eta) = 4\eta^2 - 2, \quad H_3(\eta) = 8\eta^3 - 12\eta, \quad H_4(\eta) = 16\eta^4 - 48\eta^2 + 12,$$

$$H_5(\eta) = 32\eta^5 - 160\eta^3 + 120\eta, \quad H_6(\eta) = 64\eta^6 - 480\eta^4 + 720\eta^2 - 120, \quad H_7(\eta) = 128\eta^7 - 1344\eta^5 + 3360\eta^3 - 1680\eta, \quad \cdots.$$

Please try to plot a pressure distribution ϕ for various wave modes.

Answers:
For example you can use "EXCEL".